Cell Reports
Medicine

Article

Clinical and CSF single-cell profiling of post-COVID-19 cognitive impairment

Graphical abstract

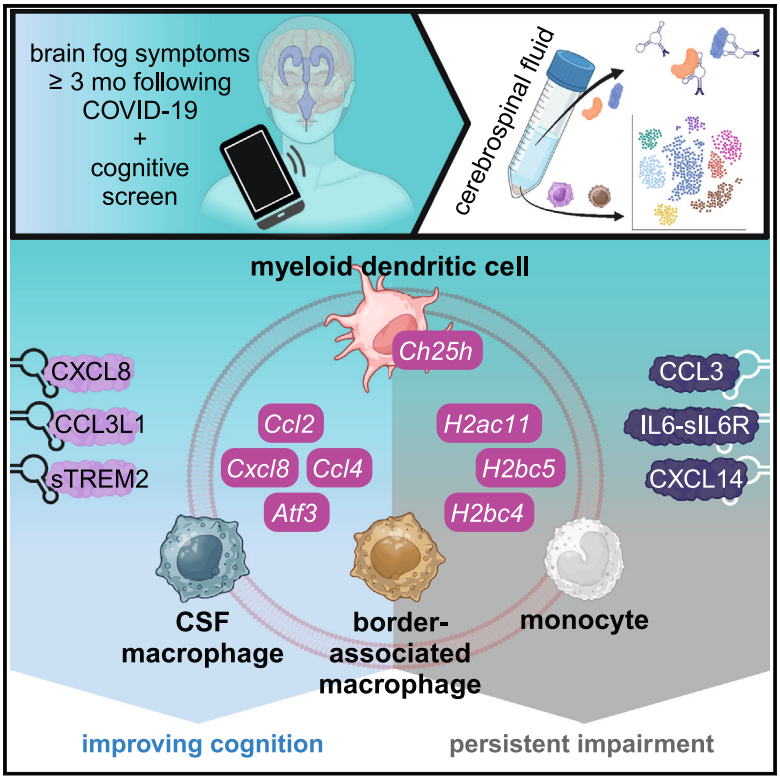

Highlights

- Improvement from post-COVID-19 cognitive impairment (CI) is slow
- Post-COVID-19 CI is molecularly distinct from Alzheimer's disease
- Post-COVID-19 CI is associated with CSF monocyte recruitment and gene alterations
- Improvement from post-COVID-19 CI is linked to greater CSF interferon responses

Authors

William T. Hu, Milota Kaluzova, Alice Dawson, ..., Mini Jomartin, Ashima Nayyar, Sabiha Hussain

Correspondence

william.hu@rutgers.edu

In brief

Clinical and cellular features of post-COVID-19 cognitive impairment remain elusive. Hu et al. show improvement from this condition to be slow and link this improvement to single-cell gene expression profiles of greater monocyte recruitment and interferon-associated responses in the cerebrospinal fluid.

Hu et al., 2024, Cell Reports Medicine *5*, 101561
May 21, 2024
https://doi.org/10.1016/j.xcrm.2024.101561

CellPress

Please cite this article in press as: Hu et al., Clinical and CSF single-cell profiling of post-COVID-19 cognitive impairment, Cell Reports Medicine (2024), https://doi.org/10.1016/j.xcrm.2024.101561

Cell Reports Medicine

CellPress
OPEN ACCESS

Article

Clinical and CSF single-cell profiling of post-COVID-19 cognitive impairment

William T. Hu,[1,2,5,*] Milota Kaluzova,[1] Alice Dawson,[1,2] Victor Sotelo,[1,2] Julia Papas,[1,2] Alexander Lemenze,[3] Carol Shu,[4] Mini Jomartin,[1] Ashima Nayyar,[1] and Sabiha Hussain[4]

[1]Department of Neurology, Rutgers-Robert Wood Johnson Medical School, New Brunswick, NJ, USA
[2]Center for Innovation in Health and Aging Research, Institute for Health, Health Care Policy, and Aging Research, New Brunswick, NJ, USA
[3]Department of Pathology and Laboratory Medicine, Rutgers-New Jersey Medical School, Newark, NJ, USA
[4]Department of Medicine-Pulmonary and Critical Care, Rutgers-Robert Wood Johnson Medical School, New Brunswick, NJ, USA
[5]Lead contact
*Correspondence: william.hu@rutgers.edu
https://doi.org/10.1016/j.xcrm.2024.101561

SUMMARY

Natural history and mechanisms for persistent cognitive symptoms ("brain fog") following acute and often mild COVID-19 are unknown. In a large prospective cohort of people who underwent testing a median of 9 months after acute COVID-19 in the New York City/New Jersey area, we found that cognitive dysfunction is common; is not influenced by mood, fatigue, or sleepiness; and is correlated with MRI changes in very few people. In a subgroup that underwent cerebrospinal fluid analysis, there are no changes related to Alzheimer's disease or neurodegeneration. Single-cell gene expression analysis in the cerebrospinal fluid shows findings consistent with monocyte recruitment, chemokine signaling, cellular stress, and suppressed interferon response—especially in myeloid cells. Longitudinal analysis shows slow recovery accompanied by key alterations in inflammatory genes and increased protein levels of CXCL8, CCL3L1, and sTREM2. These findings suggest that the prognosis for brain fog following COVID-19 correlates with myeloid-related chemokine and interferon-responsive genes.

INTRODUCTION

Memory loss, difficulties concentrating, and "brain fog" following COVID-19 (cognitive post-acute sequelae of severe acute respiratory syndrome coronavirus 2 [SARS-CoV-2] [PASC] infection) are common sources of morbidity and disability, but there are few systematic studies on these subjective complaints' neuropsychological, imaging, biological, or prognostic correlates. Findings from the UK Biobank among those with pre-COVID MRI have shown cortical gray matter atrophy on MRI following viral infection according to disease severity,[1] and other smaller post-COVID-19 series have reported changes in the deep gray nuclei,[2] brainstem,[3] and white matter tracks.[4] Mechanistic pathways proposed for these symptoms and findings—based on case studies of people with acute SARS-CoV-2 infection and neurological complications—include Alzheimer's disease (AD) pathology, direct viral neuro-invasion and viral persistence,[5] para-/post-infectious inflammatory dysregulation[6] including autoimmunity,[7] and blood-brain barrier disruption,[8] as well as psychological factors. However, it remains unclear if acute and sometimes fatal brain involvement can be extrapolated to explain prolonged cognitive symptoms in people whose initial infection was mild and self-limited.

In the US, the New York City/New Jersey area was one of the earliest regions impacted by the COVID-19 pandemic. We began tracking people with self-reported PASC symptoms in late 2020 and recruited them into a prospective registry for longitudinal standardized clinical and cognitive tracking. Within, as well as parallel to, this group, we recruited participants for detailed neuropsychological, brain MRI, cerebrospinal fluid (CSF) AD biomarkers, and CSF single-cell RNA sequencing (scRNA-seq) analysis. CSF scRNA-seq is a relatively novel method, with the largest series used to characterize pathologic conditions ranging from 3 to 15 cases.[9–11] Pooled analysis across multiple CSF and parenchymal scRNA-seq studies confirmed CSF myeloid cells to have differentially expressed genes (DEGs) representative of CNS and border tissue populations,[10] but scRNA-seq analysis can be limited by low numbers of collected cells, blood contamination, and inappropriate comparison samples. Relevant to SARS-CoV-2, CSF scRNA-seq[7] is rare compared to *in vitro*[12] or non-CSF[13–15] profiling. Mouse models of mild SARS-CoV-2 infection also showed transient (CXCL5, interferon [IFN]-γ, interleukin [IL]-6), persistent (CCL7, CXCL2), or progressive (CCL11) post-infectious elevation of CSF cytokine/chemokine, as well as white matter microglial reactivity, even in the absence of neuroinvasion.[6] Here, we collected a modest volume of CSF (15–20 mL) from people who are healthy (no confirmed COVID-19 infection, no PASC symptoms; $n = 12$) and who have cognitive PASC ($n = 16$) to determine the gene expression profiles in 15 CSF cell types associated with cognitive PASC. Leveraging the longitudinal nature of the parent study, we also sought gene expression profiles associated with persistent cognitive PASC

Please cite this article in press as: Hu et al., Clinical and CSF single-cell profiling of post-COVID-19 cognitive impairment, Cell Reports Medicine (2024), https://doi.org/10.1016/j.xcrm.2024.101561

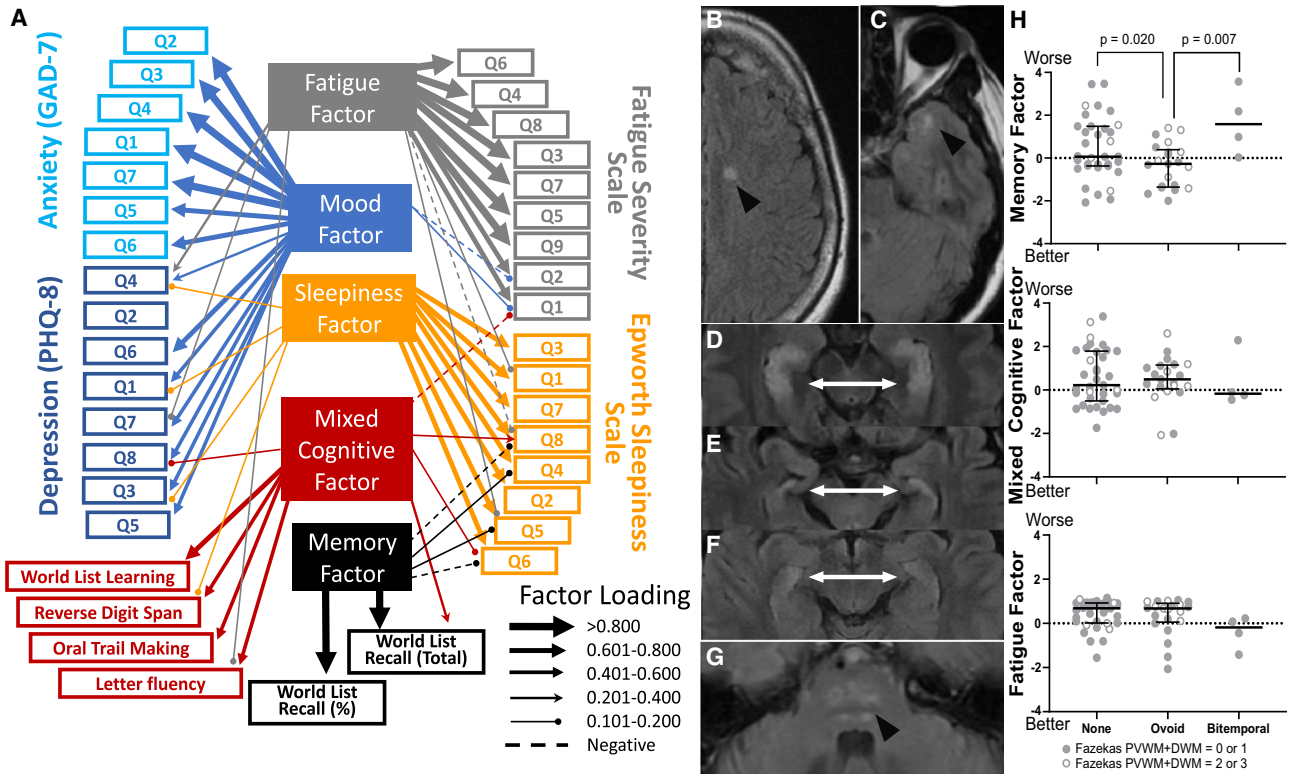

Figure 1. Clinical and MRI assessment of participants with PASC and cognitive complaints

(A) Participants with cognitive complaints were analyzed through exploratory factor analysis to determine intrinsic constructs underlying cognitive, mood (patient health questionnaire-8, PHQ-8; generalized anxiety disorder-7, GAD-7), and fatigue outcomes (n = 136 participants). Two cognitive, one mood, one sleep, and one general fatigue factor was identified, with responses to each questionnaire largely corresponding to the theoretical construct except for a common mood factor shared by PHQ-8 and GAD-7.

(B–G) MRI fluid-attenuated inversion recovery (FLAIR) analysis (n = 60 participants) revealed isolated ovoid WMH (B and C), bilateral medial temporal WMHs (D–F), and pontine WMH (G).

(H) Memory factor scores (lower score associated with less pathology/dysfunction) were lower in people with ovoid WMH than people with bitemporal WMHs or non-specific findings, including after adjusting for more typical periventricular WM (PVWM) or deep WM (DWM) changes according to Fazekas scores (p values shown are from pair-wise comparisons in regression models). There were no differences in mixed cognitive or fatigue factor scores.

vs. recovery from cognitive PASC to inform further phenotyping and treatment strategies.

RESULTS

Between February 2021 and January 2023, 211 of 311 (68%) registered patients at the Rutgers Post-COVID Recovery Clinic reported a decline in thinking or memory. 124 of these patients completed a validated brief cognitive assessment (BCA) consisting of four tests,[16] and 57% had an abnormal performance in at least one test (62% for oral trail making test, 53% for letter-guided fluency ["F"-only], 31% for reverse digit span, 13% for delayed recall of six words; 46% had two or more abnormal tests). We additionally recruited 12 participants with self-reported post-COVID brain fog from the Rutgers Cognitive Neurology Clinic or the community (136 in total), and we considered all those with abnormal performance on at least one objective test as having PASC with cognitive impairment (PASC-CI; n = 79, Figure 1; Table S1). The remaining participants with cognitive complaint but normal test scores (n = 57) are referred to as PASC with subjective cognitive concerns (PASC-SCC). Extended neuropsychological testing in a subset (n = 19, Table S2) actually showed the two groups to have similar cognitive performances, except PASC-SCC participants did better on letter-guided fluency but worse on tests performed last (word list recall) than PASC-CI participants. Because PASC-CI participants had more readily detectable cognitive dysfunction on the BCA, they were subsequently followed longitudinally for the natural history portion of the current study.

PASC-SCC and PASC-CI participants were very similar in age, gender, and pre-COVID-19 co-morbidities to PASC patients without any cognitive complaints. However, PASC-SCC and PASC-CI were both associated with greater scores for fatigue, sleepiness, depression, and anxiety than PASC participants without cognitive complaints. Exploratory factor analysis across the entire cohort identified five factors to load onto the individual cognitive scores and item-level responses to the four non-cognitive scales including the fatigue severity scale (FSS), a patient health questionnaire (PHQ-8) for depression, generalized anxiety scale 7-item (GAD-7) for anxiety, and the Epworth sleepiness

Please cite this article in press as: Hu et al., Clinical and CSF single-cell profiling of post-COVID-19 cognitive impairment, Cell Reports Medicine (2024), https://doi.org/10.1016/j.xcrm.2024.101561

scale (ESS; Figure 1; Table S3). Two factors loaded onto the cognitive scores, with one (memory factor) loading only and strongly onto delayed recall measures, while the other (mixed cognitive factor) loaded onto mostly executive function tests but also weakly onto one recall test. A common mood factor loaded onto both GAD-7 and PHQ-8, and one factor each loaded to FSS and ESS questions. These unique factors accounting for cognitive and non-cognitive functions thus support the notion of a distinct cognitive phenotype in PASC independent of mood, fatigue, or sleepiness.

MRI abnormalities are common in PASC-CI and PASC-SCC

60 participants (48 PASC-CI, 12 PASC-SCC) underwent baseline brain MRI analysis, and five major patterns of white matter hyperintensity (WMH) were identified (Table S4): none, peri-ventricular WMH(s) (Fazekas scale 0–2) with or without deep subcortical WMH(s) (Fazekas scale 0–2), isolated ovoid WMH (Figures 1B and 1C), bilateral medial temporal WMHs (Figures 1D–1F), and pontine WMH (Figure 1G). We found participants with ovoid WMHs to have more preserved memory than those with bitemporal WMH ($t = 2.785$, $p = 0.007$) as well as those without any of the COVID-type WMH ($t = 2.405$, $p = 0.020$, including after adjusting for peri-ventricular and deep WMH), but these differences were quite small. Therefore, MRI findings alone were not sufficiently predictive of cognitive or non-cognitive functions.

PASC-CI and PASC-SCC are molecularly distinct from AD

30 PASC-CI or PASC-SCC participants underwent CSF collection, and levels of established CSF AD biomarkers—including beta-amyloid 1-42 (Aβ42), total t-Tau, and p-Tau_{181}—were measured using an automated analyzer.[17] PASC participants had levels of biomarkers reflecting amyloid plaque (Aβ42) and neurofibrillary tangles (p-Tau_{181}) indistinguishable from pre-pandemic as well as post-2020 healthy control (HC; Figure 2A) participants.[18] Levels of t-Tau implicated in neurodegeneration were also normal in PASC (Figure 2B), and there was no difference between PASC-CI and PASC-SCC. In contrast, AD was associated with characteristically reduced Aβ42 levels and increased p-Tau_{181} as well as t-Tau levels. Together, these findings strongly propose that mechanisms underlying PASC-CI/PASC-SCC do not implicate amyloid and tau metabolism.

CSF and blood cells show distinct gene expression profiles

34 CSF samples (14 HCs, 15 PASC-CI, 5 PASC-SCC) were processed for scRNA-seq (Table S5), and 28 samples (82%: 12 HCs, 12 PASC-CI, 4 PASC-SCC) passed quality control for subsequent analysis. Most participants with PASC-CI (18/23) and PASC-SCC (6/7) had mild disease, which did not result in clinical visits, and only one PASC-SCC participant was briefly hospitalized (but did not require intensive care or intubation). To better characterize DEGs between CSF and peripheral mononuclear cells, two participants with PASC and two with AD had simultaneous collection of CSF and blood for parallel scRNA-seq analyses (Data S1; Figure S1). Myeloid cells showed the greatest CSF-peripheral differences with 2,530 DEGs (>2-fold change, adjusted p value [p.adj] < 0.05; Data S1), while B (44) and $CD8^+$ T (25) cells had the fewest. Known AD risk genes were among the most preferentially expressed in CSF myeloid cells (*APOE* at 4,383×, *SPP1* at 1,298×, and *TREM2* at 856×; Figure 2C).

Our workflow resulted in approximately twice as many cells per individual (total of 61,282 cells in 28 people) as the largest pervious CSF series (70,391 cells in 59 people[9]). This enrichment enabled us to identify in greater resolution CSF T and myeloid cell subtypes. CSF T cells (*Ptprc*, *Cd3e*) were classified into CD8 (*Cd8a/b*, *Ccl5*, *Plek*), effector CD8 (*Cd8a/b*, *Ccl5*, *Hopx*), natural killer (NK; *Klrb1*, *Nkg7*; low *Cd8b*, *Cd3e*), and helper cells T_H1 (*Il12rb2*, *Anxa3*, *Tbx21*, *Ifngr1*, *Ccl4*, *Eomes*), T_H2 (*Gata3*, *Mrps26*, *Lima1*, *Spint2*), and T_H17/regulatory T (T_{reg}; *Foxp3*, *Basp1*, *Tnfrsf8*) using a combination of canonical gene markers and SingleR classification to the Human Primary Cell Atlas.[19–21] Each participant's myeloid cells (median: 399.5, range: 43–1,317) were classified by unsupervised clustering into seven subpopulations (Figure S2), and comparison of standardized gene expression with prior CSF single-cell and post-mortem single-nuclei RNA-seq studies provided clues toward each cluster's composition (Figure 2D). Cells in clusters 1–3 showed features of macrophages (MPs) and microglia, but we conservatively refer to these as CSF MPs, as we could not obtain parenchymal microglia for a reference gene expression profile during CSF collection. Cluster 1 (MP1) had high expression of *Spp1*, *Trem2*, *Apoe*, *P2ry12*, and *Tmem119*, features shared by homeostatic microglia. Compared to cluster 1, cluster 2 (MP2) had higher *Spp1*, *P2ry12*, *Tmem119*, *Hexb*, *Slc2a5*, and *Ms4a7* and relatively lower *P2ry12*, *Tmem119*, and *Cx3cr1*. Cluster 3 was characterized by IFN-responsive (IR) *Isg15*, *Mx1*, *Ifit3*, and *Ifit2*, consistent with IR cells (IR-MPs) seen in mouse[22] and human[23] brains. Clusters 4 and 5 were characterized by enhanced *Lyve1* expression associated with border-associated macrophages (BAMs),[24] with higher expression of *Mrc1* (cluster 4) and *Emp3* (cluster 5).[25,26] Cluster 6 was characterized by *Cd1C*, *Fcer1A*, and *Clec10a*, consistent with CD1C+ myeloid dendritic cells (mDCs) previously identified in blood.[10,27] Finally, cluster 7's enhanced expression of *Fcn1*, *Vcan*, and *Ctss* suggests them as monocytes or monocyte-derived cells (mn) also identified in post-mortem brain single-nuclei RNA-seq and CSF.[10,23]

Comparison of collected cell numbers did not show a relationship between PASC-CI/PASC-SCC with differential regulation of any one cluster (Figure S2; Table S6). We thus next performed pseudo-bulk and pathway analysis to identify genes and biological processes associated with PASC-CI/PASC-SCC.

PASC-CI is associated with dysregulated CSF myeloid and T cell gene expression

Because high-resolution DEG characterization is a strength but also a potential limitation of scRNA-seq, we developed parallel and complementary analytical strategies to generate molecular insight into PASC-CI. We begin with pseudo-bulk analysis (single-gene level), followed by a progressive gene set enrichment analysis (GSEA)[28] approach. For each major phenotype comparison, we first performed a GSEA using the smallest MSigDB gene set (hallmark[29]) with permissive thresholds (genotype permutation) to identify overall patterns of change across different cell

Please cite this article in press as: Hu et al., Clinical and CSF single-cell profiling of post-COVID-19 cognitive impairment, Cell Reports Medicine (2024), https://doi.org/10.1016/j.xcrm.2024.101561

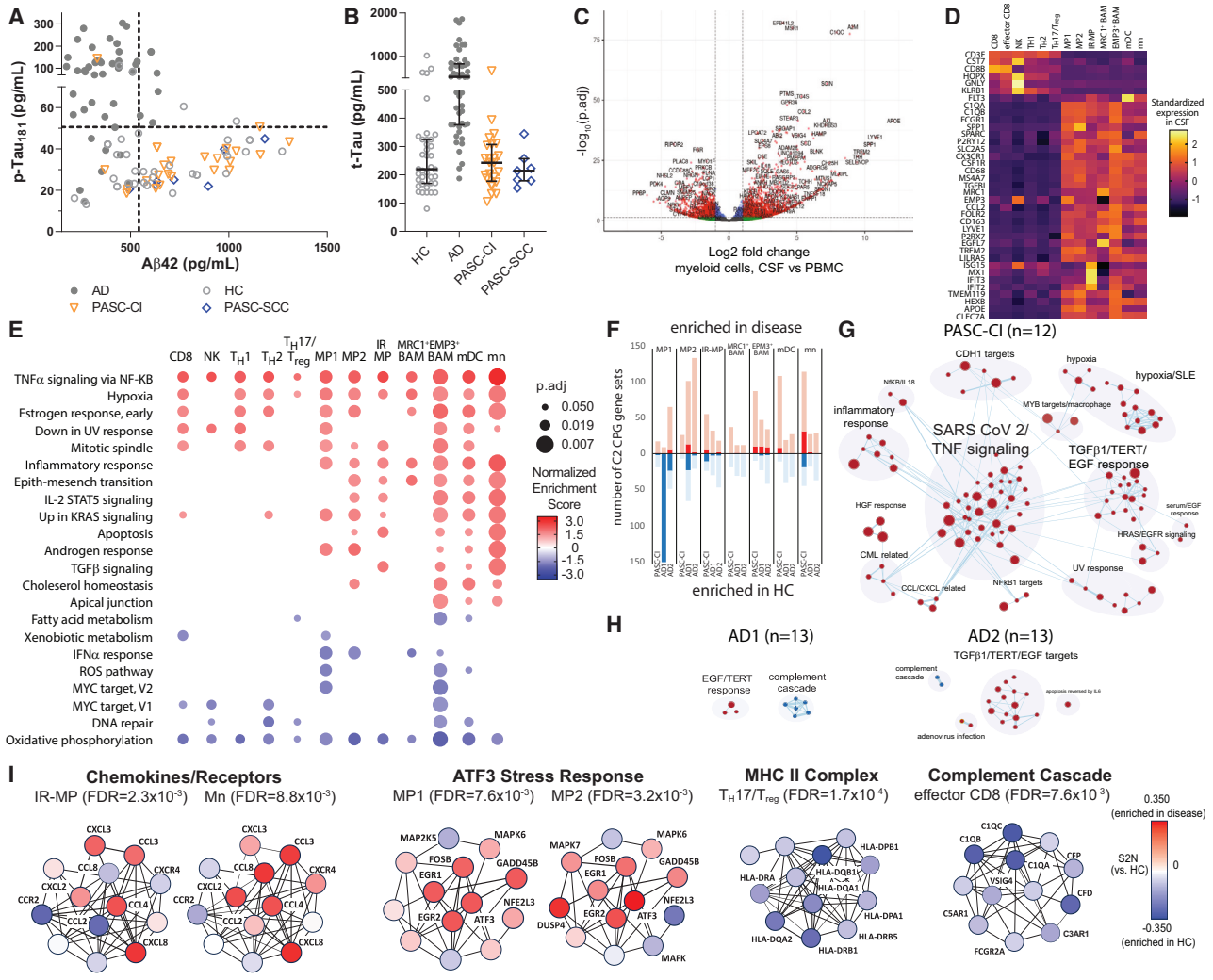

Figure 2. CSF findings in PASC-CI/PASC-SCC

(A) PASC-CI/PASC-SCC participants (n = 30) had CSF Aβ42 and p-Tau$_{181}$ levels indistinguishable from healthy control (HC) participants (n = 38) recruited before or after the pandemic began and quite different from patients with Alzheimer's disease (AD; n = 48).

(B) Levels of a more general marker of neurodegeneration (t-Tau) are also similar between PASC-CI/PASC-SCC participants and HCs (lines represent median and interquartile ranges).

(C and D) Paired CSF and peripheral blood mononuclear cell (PBMC) scRNA-seq showed distinct GE profiles according to biofluid source (C, n = 4 participants), and unsupervised cluster analysis of CSF monocytes identified seven distinct groups corresponding to previously reported CSF macrophages, border-associated macrophages (BAMs), and monocytes (D).

(E) GSEA identified EPM3+ BAMs and monocytes to be most affected in CSF, with p adj from GSEA shown.

(F) GSEA using conservative (dark) or liberal (light) thresholds showed biological processes over- (red) or under-represented (blue) in PASC-CI participants (n = 12 participants) relative to HCs (n = 12 participants) in multiple CSF myeloid cells but greater changes in PASC-CI than AD in monocytes, mDCs, and IR-MPs.

(G and H) In monocytes, PASC-CI (G) was more associated with infection-related and inflammatory processes than two similarly powered cohorts of AD (H).

(I) STRING analysis identified shared PASC-CI interaction networks involving chemokines/receptors and ATF3 stress response, as well as unique networks including downregulated major histocompatibility complex (MHC) class II genes in T$_H$17/T$_{reg}$ cells and complement cascade genes in effector CD8 cells. FDR values reflect network enrichment.

types. We then performed a GSEA using larger gene sets (C2 curated and C5 ontology) with more conservative thresholds (phenotype permutation). To improve specificity, we included 26 cases of biomarker-confirmed AD in the mild CI (MCI) or mild dementia stage recruited in parallel to HCs and PASC participants. Genes associated with PASC-CI by GSEA in multiple biological pathways (i.e., leading edge) were then examined for comparisons between HC and AD subgroups or between AD subgroups. Finally, we cross-referenced DEGs with protein-protein interaction networks to identify putative intra- and intercellular signaling cascades associated with PASC-CI.

Pseudo-bulk analysis found 97 (unadjusted $p < 0.001$) DEGs between HCs and PASC-CI participants. Three DEGs had $p < 0.05$ after false discovery rate (FDR) adjustments for multiple

Please cite this article in press as: Hu et al., Clinical and CSF single-cell profiling of post-COVID-19 cognitive impairment, Cell Reports Medicine (2024), https://doi.org/10.1016/j.xcrm.2024.101561

comparisons, and only *Ch25h* in the mDC cluster had a modest magnitude change in PASC-CI participants (1.89×) compared to HCs (Data S2). *Ch25h* is an IFN-induced gene whose mean myeloid expression in CSF is 168-fold of that in blood (Data S1). Its level was upregulated after *in vitro* SARS-CoV-2 infection and in patients with COVID-19,[30] as well as when monocytes were recruited into injured tissue.[31] More importantly, CH25H—through its product 25-hydroxycholesterol—has been directly implicated in hippocampal dysfunction during inflammation mediated by NMDA receptors.[32] Five additional DEGs (*Plek*, *Gsn*, *Apoe*, *Srgn*, and *Tcf4*, unadjusted $p < 0.001$) were previously identified as among the top 318 altered in CSF of people with acute neurological complications from COVID-19.[7]

A low number of dysregulated genes after multiple comparison adjustments could have resulted from greater clinical/etiologic heterogeneity among PASC-CI participants than among acute severe COVID-19 cases. GSEA using hallmark gene sets associated PASC-CI with greater dysregulated gene sets in myeloid cells than T cells (Figure 2E), which contrasts with the more prominent CSF NK and T cell activation in acute neurological complications of COVID-19.[7] Three CSF myeloid cell types—EMP3+ BAMs, monocytes, and mDCs—had the greatest diversity and magnitude of altered processes, with monocytes displaying enriched gene sets associated with inflammation (tumor necrosis factor [TNF]-α, IL-2, transforming growth factor β), ultraviolet exposure, and cell signaling (estrogen, KRAS) not matched by other cell types. As internal replication, we analyzed PASC-SCC ($n = 4$)—at a sample size smaller than PASC-CI but in keeping with other single-cell studies—and found that it had a similar but more muted profile to PASC-CI (Figures S3 and S4). We note enhanced—not suppressed, as in multisystem inflammatory syndrome[15]—TNF-α signaling in PASC-CI and PASC-SCC compared to HCs. Remarkably, we also observed reduction of IFN-α-related genes in PASC-CI and PASC-SCC participants compared to HCs (Figure S4), a pattern that was previously observed in plasmacytoid DCs from severe COVID-19.[33] We additionally identified 150 genes that were altered across multiple myeloid cell types at a FDR <0.05 (Data S2). Dysregulated *Ptger4* was observed in all PASC-CI CSF myeloid subtypes, while genes involved in MP activation (*Oas1*, *Nfkbiz*, *Socs1*), viral carcinogenesis/acetylation (*Gtf2b*, *Hist1h2bd*/*H2bc5*), autophagy (*Gaparap*, *Gabarapl1*), neuron-related microglia (*Tuba1a*, *Tuba1b*), or multiple pathways (*Jun*, *Rel*, *Pik3cd*, *Actg1*) were dysregulated in three or more CSF myeloid types.

To systematically contrast CSF myeloid genes dysregulated in PASC-CI with prior COVID-19-related MP scRNA-seq datasets, we performed hierarchical clustering analysis of PASC-CI gene rank scores for 123 genes previously identified to be dysregulated in MP/myeloid cells from human[34] and ferret[35] bronchoalveolar lavage fluid (BALF), mouse brains following pulmonary SARS-CoV-2 infection,[6] hamster olfactory bulb following infection,[36] and human peripheral blood.[37] This gave rise to eight gene clusters. Clusters 1 (*Atf3*, *Ccl3*, *Cxcl8*, *Il1b*) and 2 (*Ccl4*, *Dusp6*, *Ier2*, *Adrb1*, *Sgk1*) were enriched in multiple CSF myeloid subtypes from PASC-CI, BALF M1 MPs from COVID-19 BALF, and differentiated BALF M1 in ferret COVID-19 infection but downregulated in chemokine-expressing MPs in mouse brains 7 days post-infection (Figure S5). These cells together demonstrate a microglial phenotype (*Atf3*, *Ccl3*, *Ccl4*, *Il1b*) observed in aged brains[22] and humans. Clusters 3–5 had genes that were differentially enriched in CSF myeloid subtypes from PASC-CI (e.g., cluster 3 in IR-MP, clusters 4 and 5 in mDCs and mn) but generally enriched across human specimens and animal models. These three clusters had divergent dysregulation of several injury-responsive microglial genes including those upregulated in demyelination-recruited microglia (cluster 3 genes of *Rsad2* and *Cxcl10*, cluster 4 genes of *Ccl2*, *Ctsl*, and *Spp1*) or non-specifically downregulated in injury-responsive microglia (cluster 5 genes of *Apoe*, *Mx1*, *Ifi44*, and *Ifit3).* Cluster 6 contained genes involved in viral entry (*Fcn1*, *Vcan*, *Clec4d*, *Oas2*, *Cd300lf*) downregulated in PASC-CI despite their general enrichment in all other infectious and post-infectious samples, while clusters 7 and 8 genes were more similar between HCs and PASC-CI participants. Hence, while they shared some features with acute or peri-infectious microglia/MPs, CSF cells in PASC-CI showed aging, demyelination-related, injury-responsive, and suppressed pro- as well as anti-viral phenotypes.

GSEA using C2 (including gene sets altered in human or *in vitro* SARS-CoV-2 infections) again showed EMP3+ BAMs, mDCs, and monocytes to have the highest number of dysregulated gene sets (Figure S6; Data S4 and S5). To maximize the specificity of this analysis, we performed parallel GSEAs in two AD subgroups ($n = 13$ each compared with HCs). Compared to PASC-CI, AD was associated with larger number of dysregulated gene sets in two CSF MP cells (MP1 and MP2) but fewer in monocytes and—to a more modest degree—mDCs (Figure 2F). Phenotype permutation using C2 only identified one gene set related to SARS-CoV-2 infection, but the more permissive genotype permutation showed leading edges of *Cxcl2*, *Cxcl8*, *Cxcl3*, *Ier3*, and *Tnfaip3* (99, 94, 82, and 51 edges), which, on average, were seen in 7, 5, 13, and 3.5 edges in two similarly powered AD subgroups. Many of these genes were upregulated in acute COVID-19,[38] and the top unique PASC-CI leading-edge genes included other acute SARS-CoV-2 genes including *Ccl3*, *Ccl4*, *Gadd45a*, *Plaur*, *Sod2*, and *Cdkn1a*.[39–41]

PASC-CI is associated with dysregulated network involving Ccl3/Ccl4 and their repressor Atf3

Because our PASC-CI participants underwent CSF collection many months (range: 3–18) after their initial SARS-CoV-2 infection, persistent DEGs resembling acute or subacute infection were unexpected. These findings could have resulted from the GSEA's reliance on co-expressed genes with limited information from expected autocrine/paracrine signaling among myeloid cells. We thus next examined for the presence of interacting protein clusters in PASC-CI using STRING 12.0.[42] STRING clustering identified two network changes affecting multiple cell types in PASC-CI but not in AD: chemokines/receptors with hub genes of *Cxcl8*, *Cxcl2*, *Cxcl3*, *Ccl3*, *Ccl4*, and *Ccl8* and enhanced host-pathogen interactions in human coronaviruses with hub genes of *Atf3*, *Jun*, *Fosb*, *Gadd45b*, *Egr1*, and *Map2k5* (Table S7). Chemokine/receptor gene networks in IR-MP cells (FDR = 0.0023), mDCs (FDR = 0.0016), and mn cells (FDR = 0.0088) showed enrichment of chemoattractant genes *Ccl3* and *Ccl4* without accompanied enrichment in their receptors, *Ccr5* or *Ccr8*, consistent with recruitment of non-myeloid cells

Please cite this article in press as: Hu et al., Clinical and CSF single-cell profiling of post-COVID-19 cognitive impairment, Cell Reports Medicine (2024), https://doi.org/10.1016/j.xcrm.2024.101561

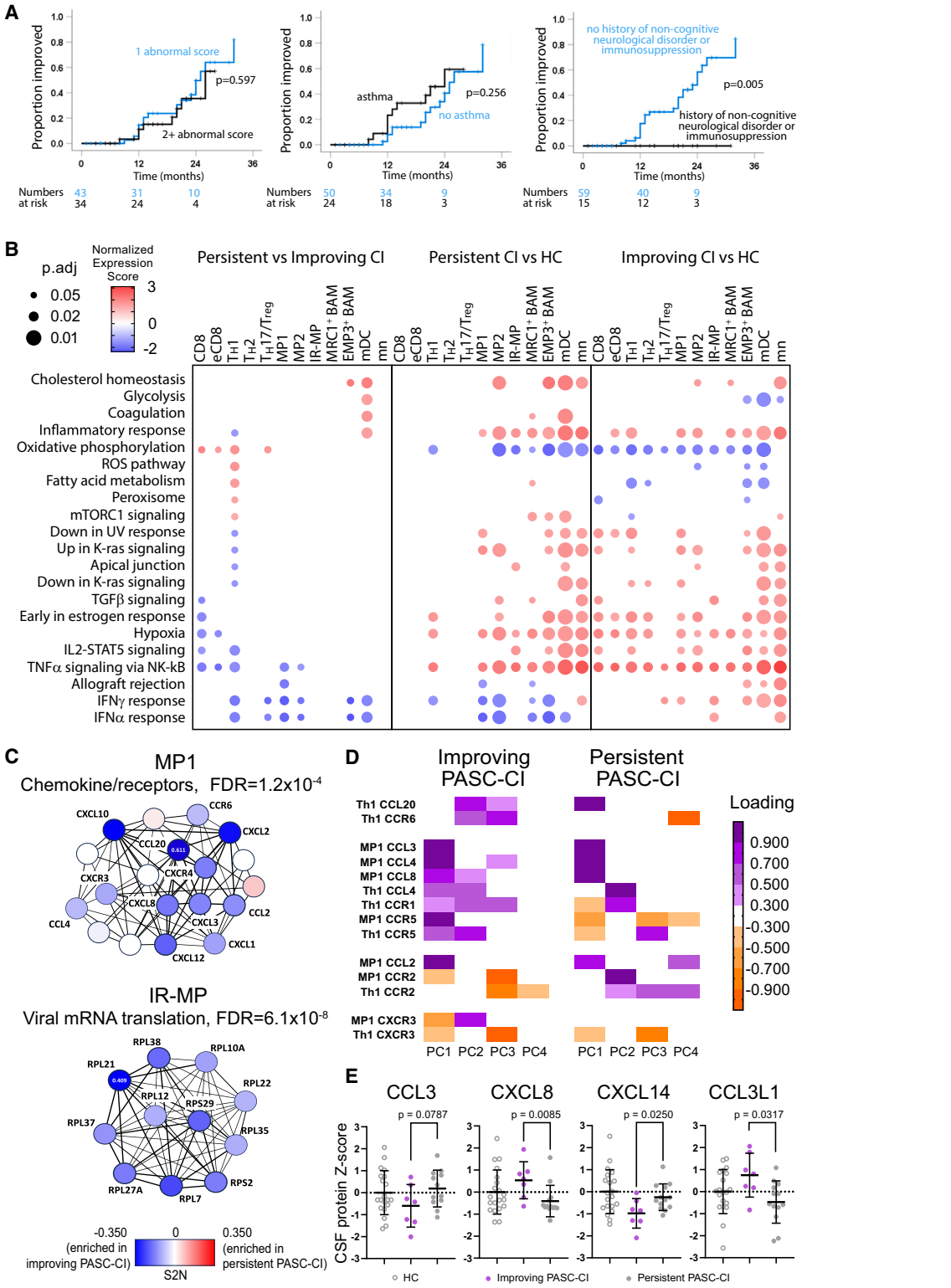

Figure 3. Factors associated with long-term PASC-CI prognosis

(A) Among 77 PASC-CI participants who consented to follow-up, recovery from PASC-CI was not associated with number of abnormal tests at baseline or common COVID-19 risk factors such as asthma but was associated with a history of immunosuppression or non-dementing neurological disorder ($p = 0.005$ by Kaplan-Meier survival analysis).

(legend continued on next page)

Please cite this article in press as: Hu et al., Clinical and CSF single-cell profiling of post-COVID-19 cognitive impairment, Cell Reports Medicine (2024), https://doi.org/10.1016/j.xcrm.2024.101561

in PASC-CI (Figure 2G). CSF MP2 cells showed similar patterns of gene dysregulation but were not identified by STRING as being significant (Figure S7). Thus, while we did not detect in the CSF a chemokine-secreting microglia subtype as was seen in mice, multiple PASC-CI CSF MPs demonstrated the same chemokine-secreting phenotype with top genes of *Ccl3*, *Ccl4*, and *Atf3*.

The other network commonly dysregulated in CSF myeloid cells has among its hub genes *Atf3* (Figure 2G). Transcription factor ATF3 is known to repress *Ccl3* and *Ccl4* but also *Ch25h* and *Ifit2*/*Ifit3*. The relative enrichment of *Ccl3*/*Ccl4* network genes (IR-MPs, mn), their repressor network (MP1, MP2, EMP3+ BAMs), or both (mDCs) thus characterizes the functional state of each cell type in PASC-CI. Extending STRING analysis to T cells in our samples additionally showed suppressed major histocompatibility complex II genes in effector CD8 cells and repressed complement cascade genes in T_H17/T_{reg} cells. Altogether, these profiles suggest that PASC-CI associates with activated chemokines and their regulatory pathways in CSF MPs but suppress T cell functions.

Improvement from PASC-CI is slow and associated with enriched chemokine/ribosomal network genes

63 PASC-CI participants had at least one longitudinal follow-up (median: 9 months after the baseline testing, range: 3–23) with the same short cognitive battery. Kaplan-Meier analysis estimated 46% of the participants to have normal testing by 24 months following the initial infection, suggesting a very long recuperation phase. The recovery curves did not differ according to the number of abnormal tests or common COVID-19 risk factors, but we found virtually no recovery among people with a common, pre-COVID neurological diagnosis (e.g., migraine, seizure) or immunosuppressive therapy (e.g., methotrexate for rheumatoid arthritis; Figure 3).

Among 12 PASC-CI participants who underwent baseline CSF scRNA-seq analysis, five (42%) had symptomatic improvement in follow-up. Pseudo-bulk analysis showed that, compared to HCs, persistent PASC-CI (n = 7) was associated with higher *Ch25h* and *Haus2* in mDCs ($\log_2$(fold change) [$\log_2$(FC)] of 2.46 and 2.02, p.adj = 0.0003 and 0.0099), higher *Srgn* in MRC1+ BAMs ($\log_2$(FC) of 1.31, p.adj = 0.0036), and lower *Ighg3* in T_H17 cells ($\log_2$(FC) of −0.46, p.adj = 4.7×10^{-9}; Data S6). Despite the greater level of IFN-stimulated *Ch25h* in those with persistent PASC-CI, GSEA (hallmark gene sets, genotype permutation) only showed enriched IFN-α and IFN-γ gene sets in improving PASC-CI but not in persistent PASC-CI (Figures 3D and 3E). This was supported by the association of chemokine/receptor network enrichment in improving PASC-CI involving not only repair-associated *Cxcl2* and *Cxcl8* but also homeostatic chemokines *Ccl20*, *Cxcl10*, and *Cxcl12*,[43] as well as their receptors *Ccr6*, *Cxcr3*, and *Cxcr4* (FDR = 0.00012 in MP1 and 0.007 in MRC1+ BAMs; Figures 3C; Table S8). GSEA and STRING additionally identified inflammatory/IFN signaling genes in Th1 cells of improving PASC-CI, in keeping with their paracrine activation via microglial chemokines (Figure 3D). By comparison, GSEA according to time since COVID-19 (<1 year, ≥1 year) did not reveal significantly altered pathways in myeloid or T cells. What's more, ribosomal genes (hub of *Rpl35*, *Rpl37*, *Rpl38*, and *Rpl7)* were enriched in improving PASC-CI participants by both GSEA and STRING but not in any of the six paired-AD comparisons (Table S8). These housekeeping proteins are necessary for host mRNA translation, but RNA viruses—including SARS-CoV-2—also utilize them for viral protein translation.[44] CSF MP enrichment in pro-inflammatory chemokines and ribosomal machinery was thus associated with better PASC-CI prognosis.

PASC-CI prognosis is associated with protective CSF inflammatory protein profiles

Since a number of chemokines and their corresponding receptors (*Ccl20* and *Ccr6*; *Cxcl10* and *Cxcr3*; *Ccl3*/*Ccl4*/*Ccl8* and *Ccr5*/*Ccr8*) were identified as differentially enriched according to PASC-CI prognosis, we performed exploratory principal-component analysis (PCA) to identify altered ligand-receptor relationships in MP1 and Th1 cells (both identified by GSEA and STRING). Whereas improving and persistent PASC-CI shared some of the first PC consisting of MP1 *Ccl2*/*Ccl3*/*Ccl4*/*Ccl8*, we observed two key differences: *Ccl20* and its receptor *Ccr6* loaded onto the same PC only in improving PASC-CI and *Ccr5* loaded positively onto its ligand PC (*Ccl3*/*Ccl4*/*Ccl8*; feedforward) in improving PASC-CI but negatively (feedback) in persistent PASC-CI (Figure 3D).

To extend the above transcriptomic findings, we measured levels of 121 inflammatory proteins related to IFN and TNF-α pathways as well as the neurofilament light chain (NfL) in CSF of HCs (n = 19) and participants with PASC-CI (n = 30) using a custom CSF proteomic array (SomaLogic, Boulder, CO, USA; Table S8). We first focused on 11 chemokines in the *Ccl3*/*Ccl4* network (CCL2, CCL3, CCL5, CCL8, CCL15, CCL3L1, CXCL8, CXCL9, CXCL13, CXCL14, TNF-α). Quite different from our earlier and others' work on acute neurological complications of SARS-CoV-2,[45,46] we found no group-level difference between PASC-CI participants and HCs. We extended this analysis to additional analytes assessed in mouse CSF 7 weeks following pulmonary SARS-CoV-infection[6] and also did not find differences between PASC-CI participants (n = 23) and HCs (n = 20) in nine analytes (IL-2, IL-4, IL-5, IL-6, IL-10, IL-18, CXCL2, CXCL10, VEGF). This can result from heterogeneity among PASC-CI participants, mixed chemokine regulations among cell types, or ligand uptake. We thus examined the same cytokines according to PASC-CI prognosis and found better

(B) GSEA (permissive thresholds, hallmark gene sets) linked improving PASC-CI (n = 5 participants) to enriched IFN- and TNF-related genes compared to persistent PASC-CI (n = 7 participants), but both PASC-CI groups shared multiple biological processes not observed in HCs. Shown are p adj values from GSEA.
(C) STRING analysis additionally identified improving PASC-CI to be enriched in many chemokine and chemokine receptor genes, as well as viral mRNA translation/cytosolic ribosomal genes, compared to persistent PASC-CI. FDR values reflect network enrichment.
(D) PCA of chemokine and chemokine receptor genes confirmed ligand-receptor gene relationships to differ according to PASC-CI prognosis.
(E) Aptamer-based assays also confirmed CSF protein levels to differ according to PASC-CI prognosis (mean and SD are shown for protein concentrations normalized to HC levels, with p values from Mann-Whitney U tests).

Please cite this article in press as: Hu et al., Clinical and CSF single-cell profiling of post-COVID-19 cognitive impairment, Cell Reports Medicine (2024), https://doi.org/10.1016/j.xcrm.2024.101561

PASC-CI prognosis to associate with higher CSF levels of CXCL8 ($p = 0.009$) and CCL3L1 ($p = 0.035$) but lower levels of CXCL14 ($p = 0.025$) and CCL3 ($p = 0.079$; Figure 3E). The pattern of decreased CCL3 and increased CXCL8 observed in improving PASC-CI shares some features with serum chemokine profiles of moderate, but not severe, COVID-19 patients.[37] We interpret these differences in extracellular chemokine levels between improving and persistent PASC-CI at a minimum as correlates of distinct intracellular/intercellular chemokine-receptor gene relationships and as preliminary evidence for a chemokine/cytokine environment conducive to inflammation resolution.[47]

Because we have empirically demonstrated that CSF proteins form composite but reproducible clusters across healthy aging and AD,[18] we further performed PCA to identify cluster-level changes associated with PASC-CI and prognosis. Two PCs were derived: PC1 with top loading from sTNFR1, sTNFR2, and NfL (Figure 4A), consistent with our previous work in HCs and patients with AD; PC2 with top loading from sTREM2 and TNFRSF4 (both showing cross-loading) as well as TRAF4, IFNL2, and the IL-6/IL-6sR complex (Figure 4B). PC2 ($p = 0.017$) and, to a lesser degree, PC1 ($p = 0.075$) scores were higher in improving PASC-CI than persistent PASC-CI. Post hoc analysis of the top loading proteins showed improving PASC-CI to associate with greater bulk sTREM2 ($p = 0.008$) levels and persistent PASC-CI to associate with greater IL-6/IL-6sR complex levels ($p = 0.020$). Because sTREM2, sTNFR1, and sTNFR2 are all markers of regulatory/feedback function in neuroinflammation and their elevated levels are associated with better prognosis in AD, their association with improving PASC-CI in the setting of cellular *Ccl3/Ccl4* gene network enrichment is most consistent with a regulated pro-inflammatory process.

DISCUSSION

PASC has overtaken acute encephalitis, encephalopathy, and stroke as the primary neurological complication of SARS-CoV-2 infection. Similar to other RNA viruses,[48–50] viral gene products have been challenging to detect in the CNS of people with acute as well as chronic neurological syndromes.[45] A recent study found positive CSF antibody titers in three out of 12 participants with PASC,[51] but only half of the group had abnormal screening cognitive scores. Here, we report PASC-CI to have cognitive deficits independent from depression and anxiety symptoms, to be molecularly distinct from AD, and to associate with dysregulated IFN- and chemokine-related genes a median of 9 months following their initial COVID-19 infection. These CSF cellular gene expression changes partially recapitulate molecular networks altered by SARS-CoV-2 *in vitro,* in human BALF, and in hamster and ferret models of acute infection. Yet, we identified key differences, including upregulated *Ch25h* consistent with monocyte recruitment to injury, opposite profiles from mouse microglia 7 days post-pulmonary SARS-CoV-2 infection, more modest and selective dysregulation in genes previously implicated in demyelination and injury responses, and downregulation of genes implicated in viral entry. We further identified better PASC-CI prognosis to correlate with greater upregulation of *Ccl2/Ccl4/Cxcl8* and higher bulk CSF levels of CXCL8, CCL3L1, and sTREM2. These findings provide strong support for the inflammatory basis of PASC-CI, highlight key network-level gene/protein alterations linked to PASC-CI outcomes, and provide a template of dysregulated pathways for animal models of PASC-CI.

Several of the CSF cell types have been broadly observed in prior human CSF or brain scRNA-seq work. Based on a larger yet safe volume of CSF collection (consistent with national studies such as the Alzheimer's Disease Neuro-imaging Initiative and Parkinson's Progression Marker Initiative), we characterized a greater number of cells and afforded the exclusion of samples with low cell count or quality. The consistent phenotyping of CSF cells using single-cell techniques is evolving, yet normalization of gene expressions across sufficient CSF myeloid cells allowed us to match unsupervised clustering outcomes to biologically meaningful cell types including CSF MPs, BAMs, mDCs, and monocytes. In our experience, scRNA-seq has been more reliable than fluorescence-activated cell sorting to identify cellular subgroups, and future simultaneous scRNA-seq with epitope mapping[52] may be necessary to confirm our clustering- and knowledge-based subtyping. Consistent with the example we presented, we anticipate only occasional correlation between single-cell-level gene expression and bulk CSF protein levels. While a sufficiently large cohort may begin to identify cell types most responsible for these CSF proteins, these findings support the complementary analysis of cell-specific DEGs and bulk CSF protein levels to best inform disease mechanisms and biomarker development.

An important observation here is that, compared to persistent PASC-CI, PASC-CI with later recovery was associated not only with greater activation of TNF-α and IFN-γ responses but also reduced or reversed relationships between a number of chemokines and their receptors (e.g., *Ccl20-Ccr6*, *Ccl3/4/8-Ccr5*). Analysis according to PASC-CI prognosis also reduces confound from co-existing mood disorders. We thus interpret PASC-CI outcomes to involve more than different extents of the same biological processes and to involve different autocrine/paracrine signaling. It is worth mentioning that we were only able to identify certain myeloid and T cell subgroups in the CSF, and our analysis could not account for parenchymal microglial cells not detectable in the CSF or cells too few in number (e.g., B cells) for scRNA-seq. A deeper characterization of distinct chemokines' and receptors' contributions to CSF bulk protein levels will require larger cohorts and more sophisticated modeling, but our findings of altered CSF CXCL8, CXCL14, CCL3L1, and CCL3 levels provides support for implicating this network in PASC-CI. We also correlated PASC-CI prognosis with CSF sTREM2 levels and, through PCA, sTNFR1/sTNFR2 levels, in keeping with previous observations in AD[18,53]—despite PASC-CI's many molecular distinctions from AD. A combination of proteins specific to improving PASC-CI and more generalized to better neurological outcomes may thus serve as potential biomarkers for PASC-CI prognosis, although this warrants future prospective testing.

A number of factors may account for DEG differences between PASC-CI CSF myeloid cells and other nervous tissue sources for scRNA-seq. First, it remains unknown whether persistent chemokine/cytokine alterations in the brain following

Please cite this article in press as: Hu et al., Clinical and CSF single-cell profiling of post-COVID-19 cognitive impairment, Cell Reports Medicine (2024), https://doi.org/10.1016/j.xcrm.2024.101561

CellPress
OPEN ACCESS

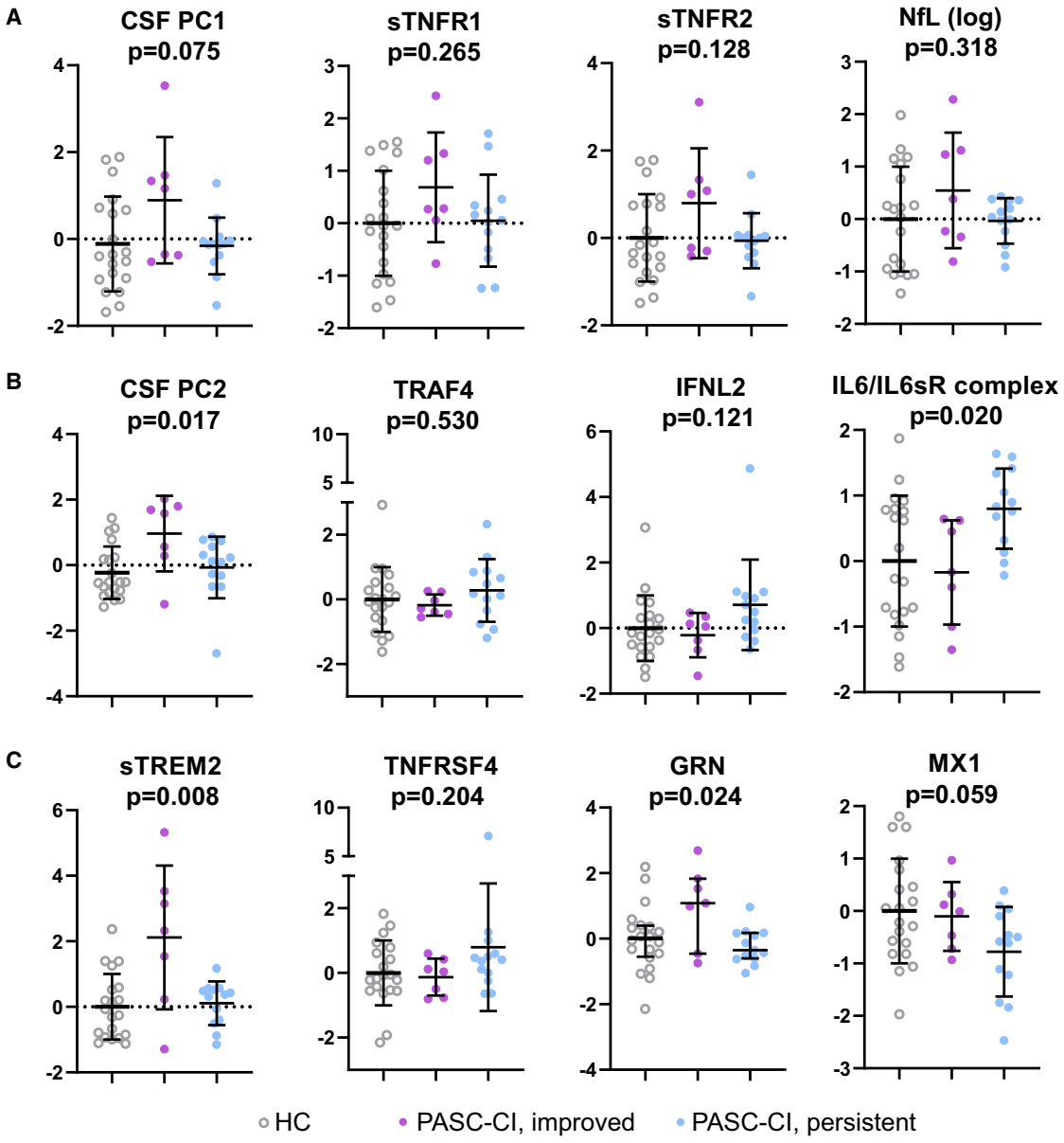

Figure 4. CSF inflammatory proteomic profiles in PASC-CI according to prognosis

PCA in 118 CSF inflammatory proteins from 19 HCs to 30 PASC-SCC/PASC-CI (20 PASC-CI participants with long-term follow-up) participants identified two PCs, which accounted for 99.6% of the variance. *p* values from ANOVA are shown.

(A) The top proteins in the first PC consisted of sTNFR1-related proteins (sTNFR1, sTNFR2) and a common marker of neurodegeneration (neurofilament light chain, NfL).

(B) The top proteins in the second PC consisted of TRAF4, IFNL2, and IL-6/IL-6sR complex.

(C) Several proteins loaded onto both PCs, including sTREM2, TNFRSF4, and progranulin (GRN), while five (such as MX1) did not load onto either PC.

Shown are CSF PC scores or Z-transformed protein concentrations using HC participants' mean and standard deviation (post hoc difference between HCs and participants with improved PASC-CI for PC2, sTREM2, and progranulin and between HCs and participants with persistent PASC-CI for IL-6/sIL-6R and MX1). Lines represent mean and standard deviations.

SARS-CoV-2 clearance adequately model human PASC-CI. Elevated *Ch25h* is consistent with continued monocyte recruitment to injured tissue, and our CSF myeloid data share greater similarities in key genes (*Akt3*, *Ccl3*, *Ccl4*, *Dusp6*) with MPs in acute SARS-CoV-2 infection than with post-recovery changes.

Second, we note that many of the IR genes (*Mx1*, *Ifi44*, *Ifi44l*, *Isg15*) previously implicated in SARS-CoV-2 viral containment and clearance[54,55] were downregulated in multiple myeloid cells and especially in MRC1+ BAMs. Whereas IR genes are generally known to be upregulated in acute infections, their expression

remains elevated in brains with HIV-associated neurocognitive disorders.[56] Their downregulation is thus noteworthy in the context of a viral illness, especially since it is associated with worse prognosis (Figure 3B). This downregulation has been observed in post-mortem AD brains[56] and in microglia from chronically stressed mice.[57] PASC-CI models may need to consider incorporating both viral infection and chronic stress, even though the prevalence for diagnosed mood disorders in our PASC-CI cohort is low (Table S1). Lastly, parenchymal and CSF-derived myeloid cells could demonstrate different DEG patterns in PASC, even though significant parallels have been identified in other neurological conditions.[10,58]

Limitations of the study

At the cost of greater generalizability, we performed high-resolution cognitive and molecular characterization in a small, non-random subset of people with PASC-CI with the following limitations. PASC-CI remains difficult to characterize due to the fatiguing nature of typical studies such as neuropsychological testing and MRI, and recruitment from outpatient clinics and communities may bias our results toward those with milder PASC-CI. Findings here should thus be replicated in participants determined to have PASC-CI in a population-based study such as the ongoing New Jersey Population Health Cohort at our institution. We could not determine if some WMH changes were present before or sustained during COVID-19, nor could we obtain viral load information on people who had COVID-19 before commercial RT-PCR was available or who underwent antigen testing. We were unable to fully confirm the identify of MP1, MP2, and IR-MPs as microglia or dura/choroid plexus-related MPs. We could not completely eliminate the possibility that some gene- or protein-level alterations were caused by another PASC syndrome such as depression, even though analysis according to PASC-CI prognosis largely identified the same pathways implicated in PASC-CI. We also did not measure all protein products of dysregulated genes including CCL4 and a proposed biomarker for PASC-CI, CCL11,[6] but our observation that CSF protein levels were more influenced by PASC-CI prognosis than the presence of CI suggests PASC-CI to have relatively less bulk protein alteration than acute or post-acute neurological complications of SARS-CoV-2. For these reasons, our findings should be viewed as hypothesis generating. Due to the small sample size, we did not analyze whether each brain MRI FLAIR pattern associated with cell-specific DEGs or CSF bulk protein changes. Nevertheless, pseudo-bulk analysis identified a greater number of DEGs after segregating PASC-CI according to long-term prognosis. This observation lends further support to subtyping PASC-CI according to longitudinal outcomes, as was done in early investigations of MCI, while the normal levels of CSF AD biomarkers and NfL reported here should obviate further plasma studies on these proteins in PASC.

STAR★METHODS

Detailed methods are provided in the online version of this paper and include the following:

SUPPLEMENTAL INFORMATION

Supplemental information can be found online at https://doi.org/10.1016/j.xcrm.2024.101561.

ACKNOWLEDGMENTS

This study is funded by NIH R01 AG 054046, Rutgers Biomedical and Health Sciences, and the TMCity Foundation.

AUTHOR CONTRIBUTIONS

W.T.H. was responsible for conception/design the study; W.T.H., M.K., A.D., V.S., J.P., A.L., C.S., M.J., A.N., and S.H. were responsible for acquisition, analysis, and interpretation of data; W.T.H., M.K., and A.L. were responsible for drafting the work; and A.D., A.N., and S.H. were responsible for critical revision of the work for important intellectual content. All authors have given final approval for the version submitted and agree to be accountable for all aspects of the work.

DECLARATION OF INTERESTS

W.T.H. has served as a consultant to ViveBio, LLC, Biogen, Inc., Fujirebio Diagnostics, Apellis Pharmaceuticals, Hoffman-LaRoche, and AARP, Inc.; received research support from Fujirebio USA; and has a patent on CSF-based diagnosis of frontotemporal lobar degeneration with TDP-43 inclusions (assigned to Emory University), CSF-based prognosis of spinal muscular atrophy (assigned to Emory University), and CSF-based prognosis of very mild AD (assigned to Emory and Rutgers University).

Received: August 22, 2023
Revised: February 15, 2024
Accepted: April 17, 2024
Published: May 13, 2024

REFERENCES

1. Douaud, G., Lee, S., Alfaro-Almagro, F., Arthofer, C., Wang, C., McCarthy, P., Lange, F., Andersson, J.L.R., Griffanti, L., Duff, E., et al. (2022). SARS-CoV-2 is associated with changes in brain structure in UK Biobank. Nature *604*, 697–707. https://doi.org/10.1038/s41586-022-04569-5.
2. Heine, J., Schwichtenberg, K., Hartung, T.J., Rekers, S., Chien, C., Boesl, F., Rust, R., Hohenfeld, C., Bungenberg, J., Costa, A.S., et al. (2023). Structural brain changes in patients with post-COVID fatigue: a prospective observational study. EClinicalMedicine *58*, 101874. https://doi.org/10.1016/j.eclinm.2023.101874.

3. Thapaliya, K., Marshall-Gradisnik, S., Barth, M., Eaton-Fitch, N., and Barnden, L. (2023). Brainstem volume changes in myalgic encephalomyelitis/chronic fatigue syndrome and long COVID patients. Front. Neurosci. *17*, 1125208. https://doi.org/10.3389/fnins.2023.1125208.

4. Rau, A., Schroeter, N., Blazhenets, G., Dressing, A., Walter, L.I., Kellner, E., Bormann, T., Mast, H., Wagner, D., Urbach, H., et al. (2022). Widespread white matter oedema in subacute COVID-19 patients with neurological symptoms. Brain *145*, 3203–3213. https://doi.org/10.1093/brain/awac045.

5. Yang, A.C., Kern, F., Losada, P.M., Agam, M.R., Maat, C.A., Schmartz, G.P., Fehlmann, T., Stein, J.A., Schaum, N., Lee, D.P., et al. (2021). Dysregulation of brain and choroid plexus cell types in severe COVID-19. Nature *595*, 565–571. https://doi.org/10.1038/s41586-021-03710-0.

6. Fernández-Castañeda, A., Lu, P., Geraghty, A.C., Song, E., Lee, M.H., Wood, J., O'Dea, M.R., Dutton, S., Shamardani, K., Nwangwu, K., et al. (2022). Mild respiratory COVID can cause multi-lineage neural cell and myelin dysregulation. Cell *185*, 2452–2468.e16. https://doi.org/10.1016/j.cell.2022.06.008.

7. Song, E., Bartley, C.M., Chow, R.D., Ngo, T.T., Jiang, R., Zamecnik, C.R., Dandekar, R., Loudermilk, R.P., Dai, Y., Liu, F., et al. (2021). Divergent and self-reactive immune responses in the CNS of COVID-19 patients with neurological symptoms. Cell Rep. Med. *2*, 100288. https://doi.org/10.1016/j.xcrm.2021.100288.

8. Soung, A.L., Vanderheiden, A., Nordvig, A.S., Sissoko, C.A., Canoll, P., Mariani, M.B., Jiang, X., Bricker, T., Rosoklija, G.B., Arango, V., et al. (2022). COVID-19 induces CNS cytokine expression and loss of hippocampal neurogenesis. Brain *145*, 4193–4201. https://doi.org/10.1093/brain/awac270.

9. Piehl, N., van Olst, L., Ramakrishnan, A., Teregulova, V., Simonton, B., Zhang, Z., Tapp, E., Channappa, D., Oh, H., Losada, P.M., et al. (2022). Cerebrospinal fluid immune dysregulation during healthy brain aging and cognitive impairment. Cell *185*, 5028–5039.e13. https://doi.org/10.1016/j.cell.2022.11.019.

10. Ostkamp, P., Deffner, M., Schulte-Mecklenbeck, A., Wünsch, C., Lu, I.N., Wu, G.F., Goelz, S., De Jager, P.L., Kuhlmann, T., Gross, C.C., et al. (2022). A single-cell analysis framework allows for characterization of CSF leukocytes and their tissue of origin in multiple sclerosis. Sci. Transl. Med. *14*, eadc9778. https://doi.org/10.1126/scitranslmed.adc9778.

11. Farhadian, S.F., Mehta, S.S., Zografou, C., Robertson, K., Price, R.W., Pappalardo, J., Chiarella, J., Hafler, D.A., and Spudich, S.S. (2018). Single-cell RNA sequencing reveals microglia-like cells in cerebrospinal fluid during virologically suppressed HIV. JCI Insight *3*, e121718. https://doi.org/10.1172/jci.insight.121718.

12. Blanco-Melo, D., Nilsson-Payant, B.E., Liu, W.C., Uhl, S., Hoagland, D., Møller, R., Jordan, T.X., Oishi, K., Panis, M., Sachs, D., et al. (2020). Imbalanced Host Response to SARS-CoV-2 Drives Development of COVID-19. Cell *181*, 1036–1045.e9. https://doi.org/10.1016/j.cell.2020.04.026.

13. Chen, H., Liu, W., Wang, Y., Liu, D., Zhao, L., and Yu, J. (2021). SARS-CoV-2 activates lung epithelial cell proinflammatory signaling and leads to immune dysregulation in COVID-19 patients. EBioMedicine *70*, 103500. https://doi.org/10.1016/j.ebiom.2021.103500.

14. Wilk, A.J., Rustagi, A., Zhao, N.Q., Roque, J., Martínez-Colón, G.J., McKechnie, J.L., Ivison, G.T., Ranganath, T., Vergara, R., Hollis, T., et al. (2020). A single-cell atlas of the peripheral immune response in patients with severe COVID-19. Nat. Med. *26*, 1070–1076. https://doi.org/10.1038/s41591-020-0944-y.

15. Sacco, K., Castagnoli, R., Vakkilainen, S., Liu, C., Delmonte, O.M., Oguz, C., Kaplan, I.M., Alehashemi, S., Burbelo, P.D., Bhuyan, F., et al. (2022). Immunopathological signatures in multisystem inflammatory syndrome in children and pediatric COVID-19. Nat. Med. *28*, 1050–1062. https://doi.org/10.1038/s41591-022-01724-3.

16. Hu, W.T., Shelnutt, M., Wilson, A., Yarab, N., Kelly, C., Grossman, M., Libon, D.J., Khan, J., Lah, J.J., Levey, A.I., and Glass, J. (2013). Behavior matters–cognitive predictors of survival in amyotrophic lateral sclerosis. PLoS One *8*, e57584. https://doi.org/10.1371/journal.pone.0057584.

17. Kollhoff, A.L., Howell, J.C., and Hu, W.T. (2018). Automation vs. Experience: Measuring Alzheimer's Beta-Amyloid 1-42 Peptide in the CSF. Front. Aging Neurosci. *10*, 253. https://doi.org/10.3389/fnagi.2018.00253.

18. Hu, W.T., Ozturk, T., Kollhoff, A., Wharton, W., and Christina Howell, J.; Alzheimer's Disease Neuroimaging Initiative (2021). Higher CSF sTNFR1-related proteins associate with better prognosis in very early Alzheimer's disease. Nat. Commun. *12*, 4001. https://doi.org/10.1038/s41467-021-24220-7.

19. Cano-Gamez, E., Soskic, B., Roumeliotis, T.I., So, E., Smyth, D.J., Baldrighi, M., Willé, D., Nakic, N., Esparza-Gordillo, J., Larminie, C.G.C., et al. (2020). Single-cell transcriptomics identifies an effectorness gradient shaping the response of CD4(+) T cells to cytokines. Nat. Commun. *11*, 1801. https://doi.org/10.1038/s41467-020-15543-y.

20. Burt, P., Peine, M., Peine, C., Borek, Z., Serve, S., Floßdorf, M., Hegazy, A.N., Höfer, T., Löhning, M., and Thurley, K. (2022). Dissecting the dynamic transcriptional landscape of early T helper cell differentiation into Th1, Th2, and Th1/2 hybrid cells. Front. Immunol. *13*, 928018. https://doi.org/10.3389/fimmu.2022.928018.

21. Aran, D., Looney, A.P., Liu, L., Wu, E., Fong, V., Hsu, A., Chak, S., Naikawadi, R.P., Wolters, P.J., Abate, A.R., et al. (2019). Reference-based analysis of lung single-cell sequencing reveals a transitional profibrotic macrophage. Nat. Immunol. *20*, 163–172. https://doi.org/10.1038/s41590-018-0276-y.

22. Hammond, T.R., Dufort, C., Dissing-Olesen, L., Giera, S., Young, A., Wysoker, A., Walker, A.J., Gergits, F., Segel, M., Nemesh, J., et al. (2019). Single-Cell RNA Sequencing of Microglia throughout the Mouse Lifespan and in the Injured Brain Reveals Complex Cell-State Changes. Immunity *50*, 253–271.e6. https://doi.org/10.1016/j.immuni.2018.11.004.

23. Olah, M., Menon, V., Habib, N., Taga, M.F., Ma, Y., Yung, C.J., Cimpean, M., Khairallah, A., Coronas-Samano, G., Sankowski, R., et al. (2020). Single cell RNA sequencing of human microglia uncovers a subset associated with Alzheimer's disease. Nat. Commun. *11*, 6129. https://doi.org/10.1038/s41467-020-19737-2.

24. Siret, C., van Lessen, M., Bavais, J., Jeong, H.W., Reddy Samawar, S.K., Kapupara, K., Wang, S., Simic, M., de Fabritus, L., Tchoghandjian, A., et al. (2022). Deciphering the heterogeneity of the Lyve1(+) perivascular macrophages in the mouse brain. Nat. Commun. *13*, 7366. https://doi.org/10.1038/s41467-022-35166-9.

25. Goldmann, T., Wieghofer, P., Jordão, M.J.C., Prutek, F., Hagemeyer, N., Frenzel, K., Amann, L., Staszewski, O., Kierdorf, K., Krueger, M., et al. (2016). Origin, fate and dynamics of macrophages at central nervous system interfaces. Nat. Immunol. *17*, 797–805. https://doi.org/10.1038/ni.3423.

26. Van Hove, H., Martens, L., Scheyltjens, I., De Vlaminck, K., Pombo Antunes, A.R., De Prijck, S., Vandamme, N., De Schepper, S., Van Isterdael, G., Scott, C.L., et al. (2019). A single-cell atlas of mouse brain macrophages reveals unique transcriptional identities shaped by ontogeny and tissue environment. Nat. Neurosci. *22*, 1021–1035. https://doi.org/10.1038/s41593-019-0393-4.

27. Villani, A.C., Satija, R., Reynolds, G., Sarkizova, S., Shekhar, K., Fletcher, J., Griesbeck, M., Butler, A., Zheng, S., Lazo, S., et al. (2017). Single-cell RNA-seq reveals new types of human blood dendritic cells, monocytes, and progenitors. Science *356*, eaah4573. https://doi.org/10.1126/science.aah4573.

28. Mootha, V.K., Lindgren, C.M., Eriksson, K.F., Subramanian, A., Sihag, S., Lehar, J., Puigserver, P., Carlsson, E., Ridderstråle, M., Laurila, E., et al. (2003). PGC-1alpha-responsive genes involved in oxidative phosphorylation are coordinately downregulated in human diabetes. Nat. Genet. *34*, 267–273. https://doi.org/10.1038/ng1180.

29. Liberzon, A., Subramanian, A., Pinchback, R., Thorvaldsdóttir, H., Tamayo, P., and Mesirov, J.P. (2011). Molecular signatures database

(MSigDB) 3.0. Bioinformatics *27*, 1739–1740. https://doi.org/10.1093/bioinformatics/btr260.

30. Nie, X., Qian, L., Sun, R., Huang, B., Dong, X., Xiao, Q., Zhang, Q., Lu, T., Yue, L., Chen, S., et al. (2021). Multi-organ proteomic landscape of COVID-19 autopsies. Cell *184*, 775–791.e14. https://doi.org/10.1016/j.cell.2021.01.004.
31. Park, M.D., Silvin, A., Ginhoux, F., and Merad, M. (2022). Macrophages in health and disease. Cell *185*, 4259–4279. https://doi.org/10.1016/j.cell.2022.10.007.
32. Izumi, Y., Cashikar, A.G., Krishnan, K., Paul, S.M., Covey, D.F., Mennerick, S.J., and Zorumski, C.F. (2021). A Proinflammatory Stimulus Disrupts Hippocampal Plasticity and Learning via Microglial Activation and 25-Hydroxycholesterol. J. Neurosci. *41*, 10054–10064. https://doi.org/10.1523/JNEUROSCI.1502-21.2021.
33. Arunachalam, P.S., Wimmers, F., Mok, C.K.P., Perera, R.A.P.M., Scott, M., Hagan, T., Sigal, N., Feng, Y., Bristow, L., Tak-Yin Tsang, O., et al. (2020). Systems biological assessment of immunity to mild versus severe COVID-19 infection in humans. Science *369*, 1210–1220. https://doi.org/10.1126/science.abc6261.
34. Liao, M., Liu, Y., Yuan, J., Wen, Y., Xu, G., Zhao, J., Cheng, L., Li, J., Wang, X., Wang, F., et al. (2020). Single-cell landscape of bronchoalveolar immune cells in patients with COVID-19. Nat. Med. *26*, 842–844. https://doi.org/10.1038/s41591-020-0901-9.
35. Lee, J.S., Koh, J.Y., Yi, K., Kim, Y.I., Park, S.J., Kim, E.H., Kim, S.M., Park, S.H., Ju, Y.S., Choi, Y.K., and Park, S.H. (2021). Single-cell transcriptome of bronchoalveolar lavage fluid reveals sequential change of macrophages during SARS-CoV-2 infection in ferrets. Nat. Commun. *12*, 4567. https://doi.org/10.1038/s41467-021-24807-0.
36. Frere, J.J., Serafini, R.A., Pryce, K.D., Zazhytska, M., Oishi, K., Golynker, I., Panis, M., Zimering, J., Horiuchi, S., Hoagland, D.A., et al. (2022). SARS-CoV-2 infection in hamsters and humans results in lasting and unique systemic perturbations after recovery. Sci. Transl. Med. *14*, eabq3059. https://doi.org/10.1126/scitranslmed.abq3059.
37. Stephenson, E., Reynolds, G., Botting, R.A., Calero-Nieto, F.J., Morgan, M.D., Tuong, Z.K., Bach, K., Sungnak, W., Worlock, K.B., Yoshida, M., et al. (2021). Single-cell multi-omics analysis of the immune response in COVID-19. Nat. Med. *27*, 904–916. https://doi.org/10.1038/s41591-021-01329-2.
38. Zhou, Z., Ren, L., Zhang, L., Zhong, J., Xiao, Y., Jia, Z., Guo, L., Yang, J., Wang, C., Jiang, S., et al. (2020). Heightened Innate Immune Responses in the Respiratory Tract of COVID-19 Patients. Cell Host Microbe *27*, 883–890.e2. https://doi.org/10.1016/j.chom.2020.04.017.
39. Guarnieri, J.W., Dybas, J.M., Fazelinia, H., Kim, M.S., Frere, J., Zhang, Y., Albrecht, Y.S., Murdock, D.G., Angelin, A., Singh, L.N., et al. (2022). Targeted Down Regulation Of Core Mitochondrial Genes During SARS-CoV-2 Infection. bioRxiv. https://doi.org/10.1101/2022.02.19.481089.
40. Lipskaia, L., Maisonnasse, P., Fouillade, C., Sencio, V., Pascal, Q., Flaman, J.M., Born, E., Londono-Vallejo, A., Le Grand, R., Bernard, D., et al. (2022). Evidence That SARS-CoV-2 Induces Lung Cell Senescence: Potential Impact on COVID-19 Lung Disease. Am. J. Respir. Cell Mol. Biol. *66*, 107–111. https://doi.org/10.1165/rcmb.2021-0205LE.
41. Sen'kova, A.V., Savin, I.A., Brenner, E.V., Zenkova, M.A., and Markov, A.V. (2021). Core genes involved in the regulation of acute lung injury and their association with COVID-19 and tumor progression: A bioinformatics and experimental study. PLoS One *16*, e0260450. https://doi.org/10.1371/journal.pone.0260450.
42. Szklarczyk, D., Kirsch, R., Koutrouli, M., Nastou, K., Mehryary, F., Hachilif, R., Gable, A.L., Fang, T., Doncheva, N.T., Pyysalo, S., et al. (2023). The STRING database in 2023: protein-protein association networks and functional enrichment analyses for any sequenced genome of interest. Nucleic Acids Res. *51*, D638–D646. https://doi.org/10.1093/nar/gkac1000.
43. Williams, J.L., Holman, D.W., and Klein, R.S. (2014). Chemokines in the balance: maintenance of homeostasis and protection at CNS barriers. Front. Cell. Neurosci. *8*, 154. https://doi.org/10.3389/fncel.2014.00154.
44. Labeau, A., Fery-Simonian, L., Lefevre-Utile, A., Pourcelot, M., Bonnet-Madin, L., Soumelis, V., Lotteau, V., Vidalain, P.O., Amara, A., and Meertens, L. (2022). Characterization and functional interrogation of the SARS-CoV-2 RNA interactome. Cell Rep. *39*, 110744. https://doi.org/10.1016/j.celrep.2022.110744.
45. Benameur, K., Agarwal, A., Auld, S.C., Butters, M.P., Webster, A.S., Ozturk, T., Howell, J.C., Bassit, L.C., Velasquez, A., Schinazi, R.F., et al. (2020). Encephalopathy and Encephalitis Associated with Cerebrospinal Fluid Cytokine Alterations and Coronavirus Disease, Atlanta, Georgia, USA, 2020. Emerg. Infect. Dis. *26*, 2016–2021. https://doi.org/10.3201/eid2609.202122.
46. Remsik, J., Wilcox, J.A., Babady, N.E., McMillen, T.A., Vachha, B.A., Halpern, N.A., Dhawan, V., Rosenblum, M., Iacobuzio-Donahue, C.A., Avila, E.K., et al. (2021). Inflammatory Leptomeningeal Cytokines Mediate COVID-19 Neurologic Symptoms in Cancer Patients. Cancer Cell *39*, 276–283.e3. https://doi.org/10.1016/j.ccell.2021.01.007.
47. Powell, D., Tauzin, S., Hind, L.E., Deng, Q., Beebe, D.J., and Huttenlocher, A. (2017). Chemokine Signaling and the Regulation of Bidirectional Leukocyte Migration in Interstitial Tissues. Cell Rep. *19*, 1572–1585. https://doi.org/10.1016/j.celrep.2017.04.078.
48. Schildgen, O., Glatzel, T., Geikowski, T., Scheibner, B., Matz, B., Bindl, L., Born, M., Viazov, S., Wilkesmann, A., Knöpfle, G., et al. (2005). Human metapneumovirus RNA in encephalitis patient. Emerg. Infect. Dis. *11*, 467–470. https://doi.org/10.3201/eid1103.040676.
49. Veje, M., Studahl, M., Johansson, M., Johansson, P., Nolskog, P., and Bergström, T. (2018). Diagnosing tick-borne encephalitis: a re-evaluation of notified cases. Eur. J. Clin. Microbiol. Infect. Dis. *37*, 339–344. https://doi.org/10.1007/s10096-017-3139-9.
50. Tilley, P.A.G., Fox, J.D., Jayaraman, G.C., and Preiksaitis, J.K. (2006). Nucleic acid testing for west nile virus RNA in plasma enhances rapid diagnosis of acute infection in symptomatic patients. J. Infect. Dis. *193*, 1361–1364. https://doi.org/10.1086/503577.
51. Mina, Y., Enose-Akahata, Y., Hammoud, D.A., Videckis, A.J., Narpala, S.R., O'Connell, S.E., Carroll, R., Lin, B.C., McMahan, C.C., Nair, G., et al. (2023). Deep Phenotyping of Neurologic Postacute Sequelae of SARS-CoV-2 Infection. Neurol. Neuroimmunol. Neuroinflamm. *10*, e200097. https://doi.org/10.1212/NXI.0000000000200097.
52. Stoeckius, M., Hafemeister, C., Stephenson, W., Houck-Loomis, B., Chattopadhyay, P.K., Swerdlow, H., Satija, R., and Smibert, P. (2017). Simultaneous epitope and transcriptome measurement in single cells. Nat. Methods *14*, 865–868. https://doi.org/10.1038/nmeth.4380.
53. Ewers, M., Franzmeier, N., Suárez-Calvet, M., Morenas-Rodriguez, E., Caballero, M.A.A., Kleinberger, G., Piccio, L., Cruchaga, C., Deming, Y., Dichgans, M., et al. (2019). Increased soluble TREM2 in cerebrospinal fluid is associated with reduced cognitive and clinical decline in Alzheimer's disease. Sci. Transl. Med. *11*, eaav6221. https://doi.org/10.1126/scitranslmed.aav6221.
54. Pekayvaz, K., Leunig, A., Kaiser, R., Joppich, M., Brambs, S., Janjic, A., Popp, O., Nixdorf, D., Fumagalli, V., Schmidt, N., et al. (2022). Protective immune trajectories in early viral containment of non-pneumonic SARS-CoV-2 infection. Nat. Commun. *13*, 1018. https://doi.org/10.1038/s41467-022-28508-0.
55. Singh, D.K., Aladyeva, E., Das, S., Singh, B., Esaulova, E., Swain, A., Ahmed, M., Cole, J., Moodley, C., Mehra, S., et al. (2022). Myeloid cell interferon responses correlate with clearance of SARS-CoV-2. Nat. Commun. *13*, 679. https://doi.org/10.1038/s41467-022-28315-7.
56. Garces, A., Martinez, B., De La Garza, R., Roy, D., Vallee, K.A., Fields, J.A., Moore, D.J., Rodrigo, H., and Roy, U. (2023). Differential expression of interferon-induced protein with tetratricopeptide repeats 3 (IFIT3) in Alzheimer's disease and HIV-1 associated neurocognitive disorders. Sci. Rep. *13*, 3276. https://doi.org/10.1038/s41598-022-27276-7.
57. Zhang, Y., Dong, Y., Zhu, Y., Sun, D., Wang, S., Weng, J., Zhu, Y., Peng, W., Yu, B., and Jiang, Y. (2022). Microglia-specific transcriptional

repression of interferon-regulated genes after prolonged stress in mice. Neurobiol. Stress *21*, 100495. https://doi.org/10.1016/j.ynstr.2022.100495.

58. Pils, M., Rutsch, J., Eren, F., Engberg, G., Piehl, F., Cervenka, S., Sellgren, C., Troßbach, S., Willbold, D., Erhardt, S., et al. (2023). Disrupted-in-schizophrenia 1 protein aggregates in cerebrospinal fluid are elevated in patients with first-episode psychosis. Psychiatry Clin. Neurosci. *77*, 665–671. https://doi.org/10.1111/pcn.13594.
59. Patnode, C.D., Perdue, L.A., Rossom, R.C., Rushkin, M.C., Redmond, N., Thomas, R.G., and Lin, J.S. (2020). Screening for Cognitive Impairment in Older Adults: Updated Evidence Report and Systematic Review for the US Preventive Services Task Force. JAMA *323*, 764–785. https://doi.org/10.1001/jama.2019.22258.
60. Ayalon, L. (2011). The IQCODE versus a single-item informant measure to discriminate between cognitively intact individuals and individuals with dementia or cognitive impairment. J. Geriatr. Psychiatry Neurol. *24*, 168–173. https://doi.org/10.1177/0891988711418506.
61. Howell, J.C., Watts, K.D., Parker, M.W., Wu, J., Kollhoff, A., Wingo, T.S., Dorbin, C.D., Qiu, D., and Hu, W.T. (2017). Race modifies the relationship between cognition and Alzheimer's disease cerebrospinal fluid biomarkers. Alzheimer's Res. Ther. *9*, 88. https://doi.org/10.1186/s13195-017-0315-1.
62. Misiura, M.B., Howell, J.C., Wu, J., Qiu, D., Parker, M.W., Turner, J.A., and Hu, W.T. (2020). Race modifies default mode connectivity in Alzheimer's disease. Transl. Neurodegener. *9*, 8. https://doi.org/10.1186/s40035-020-0186-4.
63. Fortier-Brochu, E., and Morin, C.M. (2014). Cognitive impairment in individuals with insomnia: clinical significance and correlates. Sleep *37*, 1787–1798. https://doi.org/10.5665/sleep.4172.
64. Wharton, W., Kollhoff, A.L., Gangishetti, U., Verble, D.D., Upadhya, S., Zetterberg, H., Kumar, V., Watts, K.D., Kippels, A.J., Gearing, M., et al. (2019). Interleukin 9 alterations linked to alzheimer disease in african americans. Ann. Neurol. *86*, 407–418. https://doi.org/10.1002/ana.25543.
65. Malan, L., Smuts, C.M., Baumgartner, J., and Ricci, C. (2020). Missing data imputation via the expectation-maximization algorithm can improve principal component analysis aimed at deriving biomarker profiles and dietary patterns. Nutr. Res. *75*, 67–76. https://doi.org/10.1016/j.nutres.2020.01.001.
66. Graham, J.W. (2009). Missing data analysis: making it work in the real world. Annu. Rev. Psychol. *60*, 549–576. https://doi.org/10.1146/annurev.psych.58.110405.085530.
67. Zyla, J., Marczyk, M., Weiner, J., and Polanska, J. (2017). Ranking metrics in gene set enrichment analysis: do they matter? BMC Bioinf. *18*, 256. https://doi.org/10.1186/s12859-017-1674-0.
68. Reimand, J., Isserlin, R., Voisin, V., Kucera, M., Tannus-Lopes, C., Rostamianfar, A., Wadi, L., Meyer, M., Wong, J., Xu, C., et al. (2019). Pathway enrichment analysis and visualization of omics data using g:Profiler, GSEA, Cytoscape and EnrichmentMap. Nat. Protoc. *14*, 482–517. https://doi.org/10.1038/s41596-018-0103-9.
69. Li, W. (2009). Analyzing Gene Expression Data in Terms of Gene Sets: Gene Set Enrichment Analysis (Thesis, Georgia State University). https://doi.org/10.57709/1234133.

Please cite this article in press as: Hu et al., Clinical and CSF single-cell profiling of post-COVID-19 cognitive impairment, Cell Reports Medicine (2024), https://doi.org/10.1016/j.xcrm.2024.101561

STAR★METHODS

KEY RESOURCES TABLE

REAGENT or RESOURCE	SOURCE	IDENTIFIER
Chemicals, peptides, and recombinant proteins		
RPMI 1640 Medium, Glutamax Supplement	Gibco	61870–036
FBS	Gibco	A31605-01
Critical commercial assays		
Next GEM Chip G	10X Genomics	1000120
Next GEM Single Cell 3′ Reagent Kit	10x Genomics	PN-1000268
Lumipulse® G pTau181, total Tau, Aβ42, Aβ40	Fujirebio	231654, 231661, 231678, 231302, 231326, 231319, 231463, 231487, 231708, 231685, 231692, 231708
Custom CSF inflammatory protein aptamer panel	SomaLogic	https://somalogic.com/blog/neurology-csf-profiling/
Software and algorithms		
Source code	Github (Lemenze, Rutgers)	https://doi.org/10.5281/zenodo.10962998
Cellranger	10X Genomics	Version 6.0.1
Seurat package	Satija Lab	Version 4.2.0
DoubletFinder	Github (McGinnis, UCSF)	Version 2.0.3
scTransform	Github (Satija Lab)	N/A
UMAP	Github (McInnes)	Revision 9e299ebb
DESeq2	Bioconductor	Version 1.36.0
GSEA	UC San Diego/Broad Institute	Version 4.3.2
Cytoscape 3.10.1	Cytoscape Consoritum	Version 3.10.1
SPSS Statistics	IBM	Version 28
STRING	STRING Consortium 2023	Version 12.0.42

RESOURCE AVAILABILITY

Lead contact

Further information and requests for resources and reagents should be directed to and will be fulfilled by the lead contact, William Hu (William.hu@rutgers.edu).

Materials availability

This study did not generate new unique reagents.

Data and code availability

Single-cell RNA-seq data have been deposited in and are available from the dbGaP database under GEO: GSE241385. De-identified CSF inflammatory proteomic data have been deposited at Rutgers University Community Repository: 10.7282/00000397. They are publicly available as of the date of publication.

All original code has been deposited at github (https://github.com/MaGIC-Analytics/Hu_scRNA_COVID; https://doi.org/10.5281/zenodo.10962998) and is publicly available as of the date of publication.

Any additional information required to reanalyze the data reported in this paper is available from the lead contact upon request.

EXPERIMENTAL MODEL AND STUDY PARTICIPANT DETAILS

Ethics approval

This study was approved by the Rutgers University Institutional Review Board (IRB). Written informed consents were obtained from all participants after determination that they had capacity to grant consent using the University of California Brief Assessment of Capacity to Consent.

Please cite this article in press as: Hu et al., Clinical and CSF single-cell profiling of post-COVID-19 cognitive impairment, Cell Reports Medicine (2024), https://doi.org/10.1016/j.xcrm.2024.101561

CellPress
OPEN ACCESS

Study design and recruitment

A cross-sectional design was used for baseline demographic and clinical information, brain MRI, and CSF analyses, and a longitudinal design was used to determine cognitive trajectory and reinfection. Between February 2021 and January 2023, patients evaluated at the RPRC completed survey on demographic information (age, self-reported gender, self-reported race/ethnicity [Hispanic, Black/African American, White, East Asian, South Asian, Other]), COVID-19 history (timing, symptoms, medical care), cognitive and non-cognitive PASC symptoms, GAD-7, PHQ-8, FSS, and ESS. To protect participant anonymity, age reported in sample MRI findings (Figure 1) was randomly adjusted to be within four years of actual age.

METHOD DETAILS

Case selection for PASC-CI

Because there is no universally accepted screening tool for milder forms of cognitive impairment,[59] we developed a two-stage approach to identify those with PASC and measurable cognitive dysfunction for longitudinal follow-up. In the first stage, consecutive patients (n = 311) who registered at the RPRC were asked a single question to rate their thinking and memory compared to the previous year (“Compared to last year, how would you rate your memory and thinking at the present time?”) on a 5-point Likert scale[60] from 1 (excellent) to 5 (poor) when re-infection was rare. This question was worded based on a single question found by the Aging, Demographics, and Memory Study (related to the US Health and Retirement Study) to have similar performance as the Informant Questionnaire on Cognitive Decline in the Elderly (IQCODE) in distinguishing between normal cognition and cognitive impairment not dementia. Following the first study year, this question was re-worded (“Compared to before you had COVID-19 …”) as participants began to have PASC symptoms for longer than a year.

In the second stage, patients who endorsed a score of 3 or more were contacted by trained neuropsychometricians by telephone (to maintain social distancing) to complete a validated brief cognitive assessment (BCA).[16] This consisted of four tests based on the Philadelphia Brief Assessment of Cognition: auditory verbal learning and delayed recall of six words, maximum reverse digit span, letter-guided fluency (F only), and oral trail making test. A performance at or below a Z score of −1.5 was considered abnormal. 211 of 311 (59%) patients endorsed their memory to be less than excellent or good, and 124 (59%) patients completed the BCA. 71 (57%) of those completing the BCA had abnormal performance in at least one test, and were combined with 8 of 12 participants from non-RPRC sources who also had at least one abnormal BCA score to form the PASC-CI subgroup. Remaining participants with cognitive complaint but normal test scores (n = 57) formed the PASC-SCC subgroup. 11 of 57 (19%) patients with normal BCA and 48 of 79 (61%) patients with abnormal BCA completed brain MRI analysis.

Participants for CSF analysis all underwent a structured interview with a board-certified neurologist (WTH) as part of their study visits related to initial COVID-19 symptoms, subjective cognitive symptoms, and other neurological symptoms. 19 underwent detailed neurological examination without significant findings. MRI was performed following a protocol modified from the Alzheimer’s Disease Neuroimaging Initiative to include MP-RAGE, T2, FLAIR, and GRE (or SWI for research-only scans) sequences to evaluate for gross structural abnormality, white matter hyperintensities (WMHs), and hemorrhage.[61,62]

PASC-CI participants were included if they had no cognitive complaints prior to COVID-19; had confirmed (RT-PCR, antigen testing) COVID-19 or upper respiratory illness after exposure to people with confirmed COVID-19; no other condition known to cause cognitive symptoms (e.g., prior traumatic injury, stroke, brain tumor except incidental meningioma, neurodevelopmental disorder, schizophrenia, alcoholic dementia, Parkinson’s disease, HIV). Participants were excluded if they were hospitalized in the ICU during their initial COVID-19 to rule out potential complications from prolonged hypoxia, cardiovascular instability, or secondary infection/sepsis. Participants were additionally evaluated for on-going cognitive side effects of sedating medications (e.g., narcotic, benzodiazepine) or syndromic insomnia known to cause deficits on neuropsychological testing.[63] Participants were not excluded if they had incidental discovery of periventricular or deep WMH during the evaluation, unless they were extensive (Fazekas 3 for diffuse confluent periventricular WMH or large confluent deep WMH); if they had long-standing analgesic use (e.g., gabapentin) prior to COVID-19 with no cognitive effects; if they had sub-syndromic insomnia including episodic initial, maintenance insomnia, vivid dreaming, or unrestful sleep.

After alternate causes for cognitive impairment have been ruled out, older (50+) patients with PASC-CI and PASC-SCC were offered the option of undergoing CSF analysis to rule out young-onset AD using established CSF biomarkers. Those undergoing the procedure were invited to have their CSF samples processed for single-cell analysis (see below). Other patients and community volunteers with persistent cognitive symptoms following COVID-19 were also recruited to undergo research CSF collection. CSF was collected using a 24G atraumatic Sprotte needle in the morning (between 9a.m. and noon) into polypropylene tubes without overnight fasting requirement. After CSF collection, 20 mL of whole blood was collected into K_2-EDTA tubes for separation into buffy coat and plasma. Buffy coat samples were sent to Center for Advanced Genomics (Philadelphia, PA) for genotyping. Four participants also underwent paired PBMC single-cell analysis at the time of their CSF single-cell analysis.

For comparison of AD biomarker levels, de-identified age and gender-matched CSF samples from 33 participants with normal cognition (14 recruited before and 19 recruited after March 2020) and 45 participants with MCI/AD unrelated to COVID-19 (all recruited after March 2020) were also included. Pre-pandemic participants were recruited by the senior author (WTH) through Emory University in the Atlanta area during 2010–2020 using protocols approved by the Emory University IRB. HC participants included community-recruited older White and Black participants with normal cognition and clinical dementia rating[61,64] or younger, non-carriers from families with known frontotemporal degeneration mutations with normal cognition and neuropsychological testing.

Participants with AD were recruited from the Emory Cognitive Neurology Clinic, Emory AD Research Center, or community events in the greater Atlanta area. All Emory participants underwent the same CSF collection and processing procedure as PASC-CI participants, except CSF samples were not centrifuged to derive CSF cells for scRNASeq. Pandemic-era participants were recruited from the Rutgers Cognitive Neurology Clinic, Rutgers Center for Healthy Aging, or community events in the NYC/NJ area using IRB-approved protocols. Both Cognitive Neurology Clinics are tertiary referral centers experienced in the evaluation of neurodegenerative disorders including AD, and both research centers (Emory AAD Research Center, Rutgers Center for Healthy Aging) are experienced in recruiting healthy adults (18+) into longitudinal aging studies including CSF studies. All participants who were pregnant, undergoing active cancer treatments (immuno-, chemo-, or radiation therapy), untreated or unstable depression/anxiety/other psychiatric disorders were excluded.

Single-cell preparation

To collect cellular component for single-cell transcriptome analysis, 15–20 mL of CSF from each PASC ($n = 29$) and HC ($n = 19$) participant was centrifuged at 600 g at room temperature for 10 min immediately after collection. The supernatant was carefully removed, aliquoted, labeled, and frozen until biomarker analysis. The residual cellularity (pellet usually visible to the naked eye) was then resuspended in 500 μL Gibco RPMI 1640 Medium, Glutamax Supplement (Gibco; Cat # 61870–036) plus 10% FBS (Gibco; Cat # A31605-01), spun again at 600g for 10 min in Eppendorf tube and resuspended in ~60 μL using the same media. 43.2 μL of cell suspension was loaded onto a Next GEM Chip G (10x Genomics; Cat # 1000120, Pleasanton, CA). Single cells partitioning and barcoding were performed using the Chromium single-cell controller (10x Genomics).

For PBMC cells, BD Vacutainer CPT tubes (BD BioSciences; Cat # 363760) were used. Whole blood was centrifuged at 1800 RCF for 15 min and mononuclear cells (whitish layer just under the plasma layer) were recovered and washed 2x with PBS (CORNING; Cat # 21-040-CV). Final pellet was resuspended in the same volume of RPMI-10% FBS as was the initial blood volume. Cells were counted and 16000 were loaded onto the Next GEM Chip G. Libraries were prepared using Chromium Next GEM Single Cell 3′ Reagent Kit (10x Genomics; PN-1000268) following manufacturers' instructions.

Library quality check and single-cell sequencing

Quality check was performed on a DEDAE01443 instrument and an Agilent/2100 Bioanalyser. Libraries were sequenced using NovaSeq PE150 at 48 G of raw data per sample (Novogene, Sacramento, CA). Raw reads were barcode deconvoluted and aligned to the reference genome (GRCh38) via cellranger (v6.0.1). All subsequent processing was performed in a dockerized environment using the Seurat package (v4.2.0) blinded to any upstream group metadata. All samples with primary cellranger errors indicating library prep failures, or with final filtered cells <500 were excluded from secondary analysis. Low quality cells (cells with percentage of reads of mitochondrial origin >10%, with percentage of reads of ribosomal origin >45%, with <1000 features quantified, or with >4000 features quantified) were filtered from the dataset, predicted multiplets were removed via DoubletFinder (v2.0.3). and read counts were normalized using the scTransform method clustered according to nearest neighbors using 30 principal components, and visualized via UMAP.

CSF AD biomarker analysis

CSF AD biomarkers were measured using the automated Lumipulse platform (Fujirebio Diagnostics, Malvern, PA) as previously described.[17] Our center achieves intermediate precision of 6.7%, 7.5%, and 6.1% for Aβ42, t-Tau, and p-Tau_{181}.

CSF inflammatory protein analysis

A custom CSF inflammatory protein array was developed using proteins associated with TNF-α, interferon, and other immunological signaling pathways from the greater SomaLogic CSF panel (Table S9). CSF samples were frozen at −80°C at Rutgers until over-night shipping on dry ice to SomaLogic. Because CSF protein levels were influenced by freeze-thawing cycles during internal pilots experiments conducted by Rutgers and SomaLogic, samples were only thawed at time of analysis to minimize this effect.

QUANTITATION AND STATISTICAL ANALYSIS

Missing data

Among 136 patients screened for cognitive impairment, 9 had missing PHQ-8, and 7 of the 9 also had missing GAD-7, FSS, and ESS; 4 had missing initial COVID-19 symptoms. Patients with missing data were excluded from the baseline PCA and other association analyses, but were included in the longitudinal outcome analysis.

Analysis of baseline characteristics

All demographic and clinical data were analyzed using IBM SPSS 28 (Aramonk, NY). For baseline comparisons, Student's T-test or analysis of covariance (ANOVA) were used for continuous variables, while Chi-squared tests were used for categorical variables. EFA was used to identify intrinsic constructs underlying cognitive measures, PHQ-8, GAD-7, FSS, and ESS *in a PASC cohort*. Factor loading >0.400 while omitting cases with missing data was further confirmed with imputed missing data using expectation maximization to reduce bias.[65,66]

Please cite this article in press as: Hu et al., Clinical and CSF single-cell profiling of post-COVID-19 cognitive impairment, Cell Reports Medicine (2024), https://doi.org/10.1016/j.xcrm.2024.101561

CellPress
OPEN ACCESS

Survival analysis for PASC-CI

To determine factors associated with persistent or improving PASC-CI, we performed KM survival analysis according to number of abnormal cognitive tests, presence of abnormal MRI finding, presence of key co-morbidities predisposing one to COVID-19 (diabetes, asthma, cardiovascular disease, cancer, immunocompromised state), history of non-dementing neurological disorders (headaches, epilepsy), and history of immunosuppressant treatment if present in greater than 10% of the overall PASC-CI group.

Identification and characterization of CSF cell types and subtypes

Unsupervised cluster analysis was performed to identify CSF cell groups, and DEGs associated with each cell cluster were examined to identify T cells, myeloid cells, and B cells. Pseudobulk analysis was performed comparing myeloid cells in the CSF with PBMC-derived myeloid cells to confirm a CSF myeloid phenotype. CSF T and myeloid cells each underwent further clustering analysis to identify 6 and 7 subgroups. Markers associated with each T cell subgroup were examined to identify CD8, effector CD8, NK, T_H1, T_H2, and T_H17 cells. Because myeloid cells are less well characterized in the CSF, we first identified markers previously published to associate with CSF and brain myeloid lineages (macrophages, BAM, mDC, monocytes) and standardized their corresponding VST gene expression levels across all CSF samples. The relative expression of these published markers were then manually examined to derive the most probable myeloid cell lineage.

DEG analysis, GSEA, and STRING analysis

Group cross-comparisons for DEGs between PASC-CI (persistent as well as improved), PASC-SCC, and HC were performed via pseudobulk analysis using DESeq2 (v1.36.0). Significant DEG thresholds were defined at p.adj <0.05. Genes dysregulated across multiple myeloid subtypes were first identified by nominal $p < 0.05$ within each subtype, and probability of Type I error for co-occurrence in the given number of subtypes was calculated using binomial distribution and corrected for FDR using the Benjamini-Hochberg procedure.

For GSEA between PASC-CI and HC, read counts underwent variance normalization transformation and were matched with Hallmark gene sets in GSEA (v4.3.2; Broad Institute) using permissive conditions (1,000 gene permutations, $p < 0.001$, $q < 0.05$) to derive general pathways enriched – by absolute signal-to-noise ratio or |S2N| to balance sensitivity with specificity[67] – in PASC-CI or HC. To determine if PASC-CI involved human or *in vitro* models of SARS-CoV-2 infection, GSEA using C2 was performed using more stringent (phenotype permutation, $p < 0.05$, $q < 0.25$) criteria to identify cell types most specifically impacted by comparing the number of altered pathways relative to two separate AD cohorts ($n = 13$ each) we collected and analyzed. After mDC and monocytes were shown to undergo greater pathway alterations in PASC-CI than AD, GSEA using C2 with more permissive conditions was repeated to identify leading edge DEGs. To determine biological processes linked to PASC-CI prognosis, GSEA was performed using hallmark gene sets with permissive thresholds first, but only stringent criteria (phenotype permutation) using C2 and C5 gene sets due to the smaller subgroups. To empirically determine if leading gene sets would have arisen by chance from comparing two subgroups who were indifferent from each other, we created four matching AD groups for six pairwise comparisons. Enrichment maps were visualized, auto-annotated for clusters of similar biological themes, and then manually reviewed in Cytoscape as previously described.[68]

For comparison with prior SARS-CoV-2 infection scRNASeq datasets, top genes dysregulated in acute infection (human and ferret BALF, human serum) and post-infectious nervous tissue (mouse brain, hamster olfactory bulb) were manually collated across studies, and average S2*N* values (PASC-CI vs. HC) were used in hierarchical cluster analysis (squared Euclidean distance, Ward method) to generate clusters characterized by genes sharing dysregulation patterns within or across myeloid subtypes.

To identify protein-interaction networks dysregulated in PASC-CI, genes ranked by |S2N| for each cell type were entered into STRING using local network clusters only to avoid duplication of GSEA results.[42] While the entire range of |S2N| values were used for GSEA, we limited STRING analysis to genes with $|S2N| \geq 0.05$[69] and enriched gene sets with 15 or more nodes. When multiple pathways involving the same gene sets were identified by STRING as enriched, they were combined and represented by the median enrichment score plus its associated number of matched genes. After identification of the *Ccl3/Ccl4/Ccl8/Ccr5* network, normalized gene counts for network nodes with non-zero count for at least 70% of cases were included in two PCA: one consisting of improving PASC-CI and HC, and the other of persistent PASC-CI and HC. Four PCs were identified in each based on Eigenvalue (≥ 1) and the Scree plot shoulder rule.

CSF inflammatory protein analysis

Measured CSF levels of inflammatory proteins were analyzed through two approaches. In the first hypothesis-driven approach, levels of 11 proteins involved in the CCL3/CCL4/CCL8 network (CCL2, CCL3, CCL5, CCL8, CCL15, CCL31L, CXCL8, CXCL9, CXCL13, CXCL14, TNF; CCL4 not available) were examined according to PASC-CI prognosis via Mann-Whitney U tests, with α of 0.05 without correction for multiple comparisons. In the second discovery-based approach, we followed our previous approach to determine CSF protein PCs.[18] Briefly, each individual CSF protein was examined to assess for normal distribution across the sample cohort using Kolmogorov-Smirnov Test, and CSF proteins which did not have normal distribution were log_{10}-transformed for PCA. Six proteins (IFNα1, fractalkine, IL-17F, IFNΩ1, IL-31, YKL40) could not be normalized and were excluded from PCA (co-variance matrix, minimum eigenvalue of 1, Varimax rotation). PC scores were generated and compared using analysis of variance across the three groups (HC and two PASC-CI prognostic groups). Top loading proteins for each PC were identified and examined using ANOVA, along with representative proteins which loaded onto both or neither PC.